Guaranteed and fully robust a posteriori error estimates for conforming discretizations of diffusion problems with discontinuous coefficients

Martin Vohralík

▶ **To cite this version:**

Martin Vohralík. Guaranteed and fully robust a posteriori error estimates for conforming discretizations of diffusion problems with discontinuous coefficients. 2009. hal-00235810v3

HAL Id: hal-00235810

https://hal.science/hal-00235810v3

Preprint submitted on 27 Aug 2009 (v3), last revised 21 Jul 2010 (v4)

HAL is a multi-disciplinary open access archive for the deposit and dissemination of scientific research documents, whether they are published or not. The documents may come from teaching and research institutions in France or abroad, or from public or private research centers.

L'archive ouverte pluridisciplinaire **HAL**, est destinée au dépôt et à la diffusion de documents scientifiques de niveau recherche, publiés ou non, émanant des établissements d'enseignement et de recherche français ou étrangers, des laboratoires publics ou privés.

Guaranteed and fully robust a posteriori error estimates for conforming discretizations of diffusion problems with discontinuous coefficients*

Martin Vohralík

UPMC Univ. Paris 06, UMR 7598, Laboratoire Jacques-Louis Lions, F-75005, Paris, France
&
CNRS, UMR 7598, Laboratoire Jacques-Louis Lions, F-75005, Paris, France
e-mail: vohralik@ann.jussieu.fr

Key words: finite volume method, finite element method, finite difference method, discontinuous coefficients, harmonic averaging, a posteriori error estimates, guaranteed upper bound, robustness

Abstract

We study in this paper a posteriori error estimates for H^1-conforming numerical approximations of diffusion problems with a scalar, piecewise constant, and arbitrarily discontinuous diffusion coefficient. We derive estimators for the energy norm and the dual norm of the residual which give a guaranteed global upper bound in the sense that they feature no undetermined constants. (Local) lower bounds, up to constants independent of the diffusion coefficient, are also derived. In particular, no condition on the diffusion coefficient like its monotonous increasing along paths around mesh vertices is imposed, whence the present results are fully robust and include also the cases with singular solutions. For the energy error setting, the key requirement turns out to be that the diffusion coefficient is piecewise constant on dual cells associated with the vertices of an original simplicial mesh and that harmonic averaging is used in the scheme. This is the usual case, e.g., for the cell-centered finite volume method, included in our analysis as well as the vertex-centered finite volume, finite difference, and continuous piecewise linear finite element ones. For the dual norm setting, no such a requirement is necessary. Our estimates are based on $\mathbf{H}(\mathrm{div})$-conforming flux reconstruction obtained thanks to the local conservativity of all the studied methods on the dual grids, which we recall in the paper, together with their mutual relations. Numerical experiments confirm the guaranteed upper bound, full robustness, and excellent efficiency of the derived estimators.

1 Introduction

We consider in this paper a model diffusion problem

$$-\nabla \cdot (a \nabla p) = f \qquad \text{in } \Omega, \tag{1.1a}$$

$$p = 0 \qquad \text{on } \partial\Omega, \tag{1.1b}$$

where $\Omega \subset \mathbb{R}^d$, $d = 2, 3$, is a polygonal (polyhedral) domain (open, bounded, and connected set), a is a scalar diffusion coefficient, and f is a source term. We shall derive here a posteriori error estimates for continuous piecewise linear finite element, vertex-centered finite volume, cell-centered finite volume, and finite difference approximations of this problem.

*This work was supported by the GNR MoMaS project "Numerical Simulations and Mathematical Modeling of Underground Nuclear Waste Disposal", PACEN/CNRS, ANDRA, BRGM, CEA, EdF, IRSN, France.

A posteriori error estimates for finite element discretization of (1.1a)–(1.1b) have been a popular research subject starting from the Babuška and Rheinboldt work [8]. One may formulate the following five properties describing an optimal a posteriori error estimate: 1) deliver an upper bound on the error in the numerical solution which only uses the approximate solution and which can be fully, without the presence of any unknown quantities, evaluated (*guaranteed upper bound*); 2) give an expression for the estimated error locally, for example in each element of the computational mesh, and ensure that this estimate on the error represents a lower bound for the actual error, up to a generic constant (*local efficiency*); 3) ensure that the ratio of the estimated and actual error goes to one as the computational effort goes to infinity (*asymptotic exactness*); 4) guarantee the three previous properties independently of the parameters and of their variation (*robustness*); 5) give estimators which can be evaluated locally (*negligible evaluation cost*). Property 1) allows to give a certified error upper bound, 2) is crucial for the suitability of the estimates for adaptive mesh refinement, 3) and 4) ensure the optimality of the upper bound, and 5) guarantees that the evaluation cost will be much smaller than the cost required to obtain the approximate solution itself.

A vast amount of books and papers have been dedicated to a posteriori error estimates for finite elements. We cite in particular the books by Verfürth [45], Ainsworth and Oden [3], Neittaanmäki and Repin [33], and Repin [38], cf. also Braess [13]. Among the different types of estimators, the so-called equilibrated fluxes estimates, based on equilibration of side fluxes and construction of an $\mathbf{H}(\mathrm{div})$-conforming flux, enable under certain circumstances to deliver a guaranteed upper bound. These type of estimates are pursued, e.g., by Ladevèze and Leguillon [30], Repin [39], Destuynder and Métivet [23], Luce and Wohlmuth [32], Vejchodský [44], Korotov [28], or Braess and Schöberl [15], and can be traced back to the Prager–Synge equality [36] and the hypercircle method, cf. Synge [43]. They have also recently been shown robust with respect to the polynomial degree in [14]. Much fewer results are known for finite volume methods; we refer, e.g., to Xu *et al.* [51] and the references therein.

One particular issue is the robustness with respect to discontinuous coefficient a. Robust estimates have been derived by Bernardi and Verfürth [12], Petzoldt [35], Ainsworth [1], or Chen and Dai [22]. All these estimates are, however, based on the "monotonicity around vertices" condition on the distribution of the diffusion coefficient ([12, Hypothesis 2.7]) or a similar assumption. This condition is, unfortunately, very restrictive and in particular excludes the physically interesting cases where regions with different diffusion coefficients meet in a checkerboard pattern and where the weak solution can present singularities. Recently, Cai and Zhang [17] claimed that their estimates do not need any such a condition. This is certainly true for the error upper bound, but, unfortunately, [12, Hypothesis 2.7] is used in [17, Section 4.1] in the lower bound proof.

We try to give in this paper estimates which are as close as possible to the optimality in the sense of the five above properties. Our main purpose is to present estimates which are fully robust with respect to the discontinuities in a, and this without the "monotonicity" condition. We achieve this in two different ways. The first one needs the harmonic averaging to be used in the scheme definition, while simultaneously aligning the discontinuities of the diffusion coefficient a with a dual mesh formed around vertices; it uses the energy norm. It is based on the observation of [24] that harmonic weighting can yield robustness. The second way applies to any method of this paper and requires no alignment of the discontinuities; it is based on the introduction of a (nonlocal and not locally computable) dual norm, the dual norm of the residual. Such an approach has been pursued by Angermann [4] or Verfürth [46] in the context of robust estimates for convection–diffusion problems and by Chaillou and Suri [19] in the context of monotone nonlinear problems.

None of these approaches gives robust energy norm a posteriori error estimates for the standard finite element method, where discontinuities are aligned with the mesh elements, and we by no

means claim that these two approaches are the only and the best possibilities. We rather present them as two simple ways of obtaining robust estimates for discontinuous coefficients. The first approach of aligning the discontinuities with the dual mesh is rather unusual in the finite element method. Nevertheless, it represents a standard way of handling discontinuous coefficients in the cell-centered finite volume (finite difference) approach. We merely show that suitably interpreting the solution of the standard cell-centered finite volume method with harmonic weighting in a finite element basis gives robust energy norm estimates. The key for the robustness of the second approach is the dual norm which actually does not see the jumps in the coefficients. Estimates in this norm are also only globally, and not locally, efficient. We are, however, persuaded that they are more "physical" than the energy norm estimates (see Remark 3.8 below).

We start the paper with some preliminaries in Section 2. We then in Section 3 sketch an abstract framework, both in the energy and dual norms, show its link to the Prager–Synge equality [36], and give our a posteriori error estimates. We then discuss four different ways of defining the equilibrated flux. Section 3 is closed by comparisons of the present technique with the residual, equilibrated residual, averaging, functional, and other equilibrated fluxes estimates. The proofs of the (local) efficiency and robustness are the issue of Section 4. Up to section Section 5, we mention no particular numerical scheme. In this section, we give a list of several different H^1-conforming methods, recall some useful relations between them, and show that the derived estimates apply to all of them. Finally, numerical experiments are presented in Section 6. We consider the homogeneous Dirichlet boundary condition only for the sake of clarity of exposition; general boundary conditions can easily be taken in account, as we outline it in [50]. This paper is a detailed description of the results previously announced in [49]; some additional numerical experiments for the finite element method, together with another local minimization strategy, are then studied in [20], and extensions to the reaction–diffusion case in [21].

2 Preliminaries

We give in this section the notation and assumptions, recall some important inequalities, and finally give details on the continuous problem (1.1a)–(1.1b).

2.1 Meshes and notation

We shall work in this paper with triangulations $\mathcal{T}_h$ which for all $h > 0$ consist of closed simplices such that $\overline{\Omega} = \bigcup_{K\in\mathcal{T}_h} K$ and which are conforming (matching), i.e., such that if $K, L \in \mathcal{T}_h$, $K \neq L$, then $K \cap L$ is either an empty set or a common face, edge, or vertex of K and L. Let h_K denote the diameter of K and let $h := \max_{K\in\mathcal{T}_h} h_K$. We denote by $\mathcal{E}_h$ the set of all sides of $\mathcal{T}_h$, by $\mathcal{E}_h^{\rm int}$ the set of interior, by $\mathcal{E}_h^{\rm ext}$ the set of exterior, and by $\mathcal{E}_K$ the set of all the sides of an element $K \in \mathcal{T}_h$; h_σ stands for the diameter of $\sigma \in \mathcal{E}_h$. We finally denote by $\mathcal{V}_h$ ($\mathcal{V}_h^{\rm int}$) the set of all (interior) vertices of $\mathcal{T}_h$ and put, for $V \in \mathcal{V}_h$ and $K \in \mathcal{T}_h$, respectively, $\mathcal{T}_V := \{L \in \mathcal{T}_h;\, L \cap V \neq \emptyset\}$ and $\mathcal{T}_K := \{L \in \mathcal{T}_h;\, L \cap K \neq \emptyset\}$.

We shall also consider dual partitions $\mathcal{D}_h$ of Ω such that $\overline{\Omega} = \bigcup_{D\in\mathcal{D}_h} D$ and such that for each $V \in \mathcal{V}_h$, $V \in D_V$ for exactly one $D_V \in \mathcal{D}_h$. The notation V_D stands inversely for the vertex associated with a given $D \in \mathcal{D}_h$ and we use $\mathcal{D}_h^{\rm int}, \mathcal{D}_h^{\rm ext}$ to denote the dual volumes associated with vertices from $\mathcal{V}_h^{\rm int}, \mathcal{V}_h^{\rm ext}$, respectively. Next, $\mathcal{F}_h$ stands for all sides of $\mathcal{D}_h$ and $\mathcal{F}_h^{\rm int}$ ($\mathcal{F}_h^{\rm ext}$) for all interior (exterior) sides of $\mathcal{D}_h$. We shall always suppose that D_V lies in the interior of the polygon/polyhedron given by $\mathcal{T}_V$ for all $V \in \mathcal{V}_h$ and that $\mathcal{E}_h^{\rm int} \cap \mathcal{F}_h^{\rm int}$ has a zero $(d-1)$-dimensional Lebesgue measure. An example of such a partition is given in the left part of Figure 1; more details on different $\mathcal{D}_h$ considered will be given in Section 5 below.

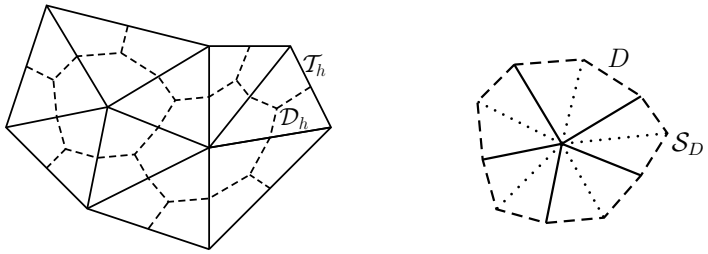

Figure 1: Original simplicial mesh $\mathcal{T}_h$ and an associated dual mesh $\mathcal{D}_h$ (left) and the fine simplicial mesh $\mathcal{S}_D$ of $D \in \mathcal{D}_h$ (right)

In order to define our a posteriori error estimates, we will need a second conforming simplicial triangulation $\mathcal{S}_h$ of Ω. The basic requirement is that the interiors of the elements of $\mathcal{S}_h$ do not intersect sides of $\mathcal{T}_h$ and $\mathcal{D}_h$ ($\mathcal{S}_h$ is a conforming refinement of both $\mathcal{T}_h$ and $\mathcal{D}_h$). For the local efficiency proofs of our estimators, we will later need the assumption that $\{\mathcal{S}_h\}_h$ are shape-regular in the sense that there exists a constant $\kappa_{\mathcal{S}} > 0$ such that $\min_{K\in\mathcal{S}_h} |K|/h_K^d \geq \kappa_{\mathcal{S}}$ for all $h > 0$. One can easily construct a local triangulation $\mathcal{S}_D$ of each $D \in \mathcal{D}_h$ as shown in the right part of Figure 1 and then put $\mathcal{S}_h := \cup_{D\in\mathcal{D}_h}\mathcal{S}_D$. We will use the notation $\mathcal{G}_h$ for all sides of $\mathcal{S}_h$ and $\mathcal{G}_h^{\rm int}$ ($\mathcal{G}_h^{\rm ext}$) for all interior (exterior) sides of $\mathcal{S}_h$. The notation $\mathcal{G}_D^{\rm int}$ stands for all interior sides of $\mathcal{S}_D$ and $\mathcal{G}_D^{\rm ext}$ for the exterior ones.

Next, for $K \in \mathcal{T}_h$, $\mathbf{n}$ will always denote its exterior normal vector; we shall also employ the notation $\mathbf{n}_\sigma$ for a normal vector of a side $\sigma \in \mathcal{E}_h$, whose orientation is chosen arbitrarily but fixed for interior sides and coinciding with the exterior normal of Ω for exterior sides. For $\sigma \in \mathcal{E}_h^{\rm int}$ shared by $K, L \in \mathcal{T}_h$ (which we denote by $\sigma_{K,L}$) such that $\mathbf{n}_\sigma$ points from K to L and a function φ, we shall define the jump operator $[\![\cdot]\!]$ by

$$[\![\varphi]\!] := (\varphi|_K)|_\sigma - (\varphi|_L)|_\sigma. \tag{2.1}$$

We put $[\![\varphi]\!]_\sigma := \varphi|_\sigma$ for any $\sigma \in \mathcal{E}_h^{\rm ext}$. We next associate with each $K \in \mathcal{T}_h$ and each $\sigma \in \mathcal{E}_K$ a weight $\omega_{K,\sigma}$ such that

$$0 \leq \omega_{K,\sigma} \leq 1 \qquad \forall K \in \mathcal{T}_h,\, \forall \sigma \in \mathcal{E}_K, \tag{2.2a}$$

$$\omega_{K,\sigma} + \omega_{L,\sigma} = 1 \qquad \forall \sigma = \sigma_{K,L} \in \mathcal{E}_h^{\rm int}, \tag{2.2b}$$

$$\omega_{K,\sigma} = 1 \qquad \forall \sigma \in \mathcal{E}_h^{\rm ext} \text{ and } K \in \mathcal{T}_h \text{ such that } \sigma \in \mathcal{E}_K. \tag{2.2c}$$

For $\sigma = \sigma_{K,L} \in \mathcal{E}_h^{\rm int}$, we define the weighted average operator $\{\!\{\cdot\}\!\}_\omega$ by

$$\{\!\{\varphi\}\!\}_\omega := \omega_{K,\sigma}(\varphi|_K)|_\sigma + \omega_{L,\sigma}(\varphi|_L)|_\sigma, \tag{2.3}$$

whereas for $\sigma \in \mathcal{E}_h^{\rm ext}$, $\{\!\{\varphi\}\!\}_\omega := \varphi|_\sigma$. Two basic choices for the weights in $[\![a]\!]_\sigma$ or $\{\!\{a\}\!\}_\sigma$ on a side $\sigma = \sigma_{K,L} \in \mathcal{E}_h^{\rm int}$ are:

$$\omega_{K,\sigma} = \omega_{L,\sigma} = \tfrac{1}{2}, \tag{2.4}$$

which corresponds to the arithmetic averaging, and

$$\omega_{K,\sigma} = \frac{a_L}{a_K + a_L}, \qquad \omega_{L,\sigma} = \frac{a_K}{a_K + a_L}, \tag{2.5}$$

which corresponds to the harmonic averaging of the diffusion coefficient a. Finally, we denote by $\{\!\{\varphi\}\!\}$ the standard average operator with $\omega_{K,\sigma} = \omega_{L,\sigma} = \frac{1}{2}$ and $\{\!\{\varphi\}\!\} := \varphi|_\sigma$ for $\sigma \in \mathcal{E}_h^{\rm ext}$. We use the same type of notation also for the meshes $\mathcal{D}_h$ and $\mathcal{S}_h$.

We shall be working below with numerical methods whose approximate solution can be represented by continuous piecewise linear functions on $\mathcal{T}_h$, with value 0 at the boundary of Ω. The basis of this space, denoted by X_h^0, is spanned by the classical pyramidal functions ψ_V, $V \in \mathcal{V}_h^{\rm int}$, such that $\psi_V(U) = \delta_{VU}$, $U \in \mathcal{V}_h$, δ being the Kronecker delta.

In what concerns functional notation, we denote by $(\cdot,\cdot)_S$ the L^2-scalar product on S and by $\|\cdot\|_S$ the associated norm; when $S = \Omega$, the index dropped off. We mean by $|S|$ the Lebesgue measure of S, by $|\sigma|$ the $(d-1)$-dimensional Lebesgue measure of $\sigma \subset \mathbb{R}^{d-1}$, and in particular by $|\mathbf{s}|$ the length of a segment $\mathbf{s}$. Next, $H^1(S)$ is the Sobolev space of functions with square-integrable weak derivatives and $H_0^1(S)$ is its subspace of functions with traces vanishing on ∂S. Finally, $\mathbf{H}(\mathrm{div}, S)$ is the space of functions with square-integrable weak divergences, $\mathbf{H}(\mathrm{div}, S) = \{\mathbf{v} \in \mathbf{L}^2(S); \nabla\cdot\mathbf{v} \in L^2(S)\}$, and $\langle\cdot,\cdot\rangle_{\partial S}$ stands for the appropriate duality pairing on ∂S.

2.2 Assumptions

We shall suppose that $f(\mathbf{x}) \in L^2(\Omega)$ and that $a(\mathbf{x})$ is a piecewise constant scalar-valued function. We in particular consider cases where a is piecewise constant on the triangulation $\mathcal{T}_h$ and cases where a is piecewise constant on the dual partition $\mathcal{D}_h$. In all cases we denote by $c_{a,K}$ and $C_{a,K}$ for all $K \in \mathcal{T}_h$ the best positive constants such that $c_{a,K} \le a(\mathbf{x}) \le C_{a,K}$ for all $\mathbf{x} \in K$. Similar notation will be used also for $D \in \mathcal{D}_h$, for $\mathcal{T}_K$, $K \in \mathcal{T}_h$, or for the entire domain.

2.3 Poincaré and Friedrichs inequalities

Let D be a polygon or a polyhedron. The Poincaré inequality states that

$$\|\varphi - \varphi_D\|_D^2 \le C_{\mathrm{P},D} h_D^2 \|\nabla\varphi\|_D^2 \qquad \forall \varphi \in H^1(D), \tag{2.6}$$

where φ_D is the mean of φ over D given by $\varphi_D := (\varphi, 1)_D/|D|$ and where the constant $C_{\mathrm{P},D}$ can for each convex D be evaluated as $1/\pi^2$, cf. [34, 11]. To evaluate $C_{\mathrm{P},D}$ for nonconvex elements D is more complicated but it still can be done, cf. [26, Lemma 10.2] or [18, Section 2].

Let $|\partial\Omega \cap \partial D| \neq 0$. Then the Friedrichs inequality states that

$$\|\varphi\|_D^2 \le C_{\mathrm{F},D,\partial\Omega} h_D^2 \|\nabla\varphi\|_D^2 \qquad \forall \varphi \in H^1(D) \text{ such that } \varphi = 0 \text{ on } \partial\Omega \cap \partial D. \tag{2.7}$$

As long as $\partial\Omega$ is such that there exists a vector $\mathbf{b} \in \mathbb{R}^d$ such that for almost all $\mathbf{x} \in D$, the first intersection of $\mathcal{B}_\mathbf{x}$ and ∂D lies in $\partial\Omega$, where $\mathcal{B}_\mathbf{x}$ is the straight semi-line defined by the origin $\mathbf{x}$ and the vector $\mathbf{b}$, $C_{\mathrm{F},D,\partial\Omega} = 1$, cf. [47, Remark 5.8]. To evaluate $C_{\mathrm{F},D,\partial\Omega}$ in the general case is more complicated but it still can be done, cf. [47, Remark 5.9] or [18, Section 3].

2.4 Continuous problem

We define a bilinear form $\mathcal{B}$ by

$$\mathcal{B}(p,q) := (a\nabla p, \nabla q) \qquad p, q \in H_0^1(\Omega). \tag{2.8}$$

The weak formulation of problem (1.1a)–(1.1b) is to find $p \in H_0^1(\Omega)$ such that

$$\mathcal{B}(p,q) = (f,q) \qquad \forall q \in H_0^1(\Omega) \tag{2.9}$$

and the corresponding energy norm is defined by

$$|||q|||^2 := \mathcal{B}(q,q) = \|a^{\frac{1}{2}}\nabla q\|^2, \qquad q \in H_0^1(\Omega). \tag{2.10}$$

Alternatively, following the approaches of Angermann [4] or Verfürth [46] and Chaillou and Suri [19] of the convection–diffusion and nonlinear settings, respectively, we will also present a posteriori error estimates in a dual norm. We will use the H^{-1} norm of the residual given by

$$|||q|||_{\#} := \sup_{\varphi \in H_0^1(\Omega)} \frac{\mathcal{B}(q,\varphi)}{\|\nabla \varphi\|}, \qquad q \in H_0^1(\Omega) \tag{2.11}$$

for this purpose.

Remark 2.1 (Energy and dual norms). The energy norm (2.10) admits a local decomposition and is easily computable. The dual norm (2.11) is a global norm and its practical computation is not obvious except of particular cases. In any case, however, it is immediate from (2.11) that there exist easily and locally computable upper and lower bounds for $|||\cdot|||_{\#}$:

$$\frac{\|a^{\frac{1}{2}} \nabla q\|^2}{\|\nabla q\|} \leq |||q|||_{\#} \leq \|a \nabla q\| \qquad \forall q \in H_0^1(\Omega). \tag{2.12}$$

In particular, the two above norms coincide when a is constant.

3 Guaranteed a posteriori error estimates

We present our main upper bound results in this section.

3.1 A simple abstract framework and its relation to the Prager–Synge theorem

We present here a simple abstract a posteriori error estimate for problem (1.1a)–(1.1b). The basic ideas can be traced back to the Prager–Synge equality [36], the hypercircle method, Synge [43], Ladevèze [29], or Repin [39].

Theorem 3.1 (Abstract energy norm a posteriori error estimate)**.** *Let p be the weak solution of problem (1.1a)–(1.1b) and let $p_h \in H_0^1(\Omega)$ be arbitrary. Then*

$$|||p - p_h||| = \inf_{\mathbf{t} \in \mathbf{H}(\mathrm{div},\Omega)} \sup_{\varphi \in H_0^1(\Omega),\, |||\varphi|||=1} \{|(f - \nabla \cdot \mathbf{t}, \varphi)| + |(a \nabla p_h + \mathbf{t}, \nabla \varphi)|\}. \tag{3.1}$$

Proof. We first notice that

$$|||p - p_h||| = \mathcal{B}\left(p - p_h, \frac{p - p_h}{|||p - p_h|||}\right)$$

by (2.10). Clearly, as $\varphi := (p - p_h)/|||p - p_h||| \in H_0^1(\Omega)$, we immediately have $\mathcal{B}(p,\varphi) = (f,\varphi)$ by (2.9). Using this we obtain, for an arbitrary $\mathbf{t} \in \mathbf{H}(\mathrm{div},\Omega)$ and employing the Green theorem,

$$\begin{aligned} \mathcal{B}(p - p_h, \varphi) &= (f,\varphi) - (a\nabla p_h, \nabla \varphi) = (f,\varphi) - (a\nabla p_h + \mathbf{t}, \nabla\varphi) + (\mathbf{t}, \nabla \varphi) \\ &\leq |(f - \nabla \cdot \mathbf{t}, \varphi)| + |(a \nabla p_h + \mathbf{t}, \nabla \varphi)|. \end{aligned}$$

From here, it is enough to note that $|||\varphi||| = 1$ and that $\mathbf{t} \in \mathbf{H}(\mathrm{div},\Omega)$ was chosen arbitrary to conclude that the right-hand side term of (3.1) is an upper bound on the left-hand side one. For the converse estimate, it suffices to put $\mathbf{t} = -a\nabla p$ and to use the Cauchy–Schwarz inequality and the fact that $|||\varphi||| = 1$. □

Similar arguments lead to the following corollary:

Corollary 3.2 (Abstract dual norm a posteriori error estimate)**.** *Let the assumptions of Theorem 3.1 be verified. Then*

$$|||p-p_h|||_{\#} = \inf_{\mathbf{t}\in\mathbf{H}(\mathrm{div},\Omega)} \sup_{\varphi\in H_0^1(\Omega),\,\|\nabla\varphi\|=1} \{|(f-\nabla\cdot\mathbf{t},\varphi)| + |(a\nabla p_h+\mathbf{t},\nabla\varphi)|\}.$$

Remark 3.3 (Relation to the Prager–Synge equality). The Prager–Synge equality [36] states, with the assumptions of Theorem 3.1, that

$$|||p-p_h|||^2 + \|a^{\frac{1}{2}}\nabla p + a^{-\frac{1}{2}}\mathbf{t}\|^2 = \|a^{\frac{1}{2}}\nabla p_h + a^{-\frac{1}{2}}\mathbf{t}\|^2$$

for any $\mathbf{t}\in\mathbf{H}(\mathrm{div},\Omega)$ such that $\nabla\cdot\mathbf{t}=f$. This result leads to

$$|||p-p_h||| \le \inf_{\mathbf{t}\in\mathbf{H}(\mathrm{div},\Omega);\,\nabla\cdot\mathbf{t}=f} \|a^{\frac{1}{2}}\nabla p_h + a^{-\frac{1}{2}}\mathbf{t}\|,$$

which is similar to (3.1). The important difference, however, is that the minimization set is here restrained to such $\mathbf{t}\in\mathbf{H}(\mathrm{div},\Omega)$ that satisfy $\nabla\cdot\mathbf{t}=f$, which is rather restrictive.

3.2 A posteriori error estimate

Starting from Theorem 3.1, we now give a fully computable a posteriori error estimate. Essential is assumption (3.2) below which enables to easily estimate the first term on the right-hand side of (3.1), related to a negative norm.

Theorem 3.4 (A guaranteed energy norm a posteriori error estimate)**.** *Let p be the weak solution of problem (1.1a)–(1.1b) and let $p_h\in H_0^1(\Omega)$ be arbitrary. Let next $\mathcal{D}_h^* = \mathcal{D}_h^{\mathrm{int},*}\cup\mathcal{D}_h^{\mathrm{ext},*}$ be a partition of Ω such that $|\partial\Omega\cap\partial D|\neq 0$ for all $D\in\mathcal{D}_h^{\mathrm{ext},*}$. Let finally $\mathbf{t}_h\in\mathbf{H}(\mathrm{div},\Omega)$ be arbitrary but such that*

$$(\nabla\cdot\mathbf{t}_h,1)_D = (f,1)_D \qquad \forall D\in\mathcal{D}_h^{\mathrm{int},*}. \tag{3.2}$$

Then

$$|||p-p_h||| \le \left\{\sum_{D\in\mathcal{D}_h^*} (\eta_{\mathrm{R},D}+\eta_{\mathrm{DF},D})^2\right\}^{\frac{1}{2}},$$

where the diffusive flux estimator $\eta_{\mathrm{DF},D}$ *is given by*

$$\eta_{\mathrm{DF},D} := \|a^{\frac{1}{2}}\nabla p_h + a^{-\frac{1}{2}}\mathbf{t}_h\|_D \qquad D\in\mathcal{D}_h^*, \tag{3.3}$$

and the residual estimator $\eta_{\mathrm{R},D}$ *is given by*

$$\eta_{\mathrm{R},D} := m_{D,a}\|f-\nabla\cdot\mathbf{t}_h\|_D \qquad D\in\mathcal{D}_h^*, \tag{3.4}$$

where

$$m_{D,a}^2 := C_{\mathrm{P},D}\frac{h_D^2}{c_{a,D}} \quad D\in\mathcal{D}_h^{\mathrm{int},*}, \qquad m_{D,a}^2 := C_{\mathrm{F},D,\partial\Omega}\frac{h_D^2}{c_{a,D}} \quad D\in\mathcal{D}_h^{\mathrm{ext},*}, \tag{3.5}$$

with $C_{\mathrm{P},D}$ the constant from the Poincaré inequality (2.6) and $C_{\mathrm{F},D,\partial\Omega}$ the constant from the Friedrichs inequality (2.7).

Proof. Put $\mathbf{t} = \mathbf{t}_h$ in Theorem 3.1. Note that, for each $D \in \mathcal{D}_h^{\mathrm{int},*}$,

$$|(f - \nabla\cdot\mathbf{t}_h, \varphi)_D| = |(f - \nabla\cdot\mathbf{t}_h, \varphi - \varphi_D)_D| \le \eta_{\mathrm{R},D}|||\varphi|||_D,$$

using (3.2), the Poincaré inequality (2.6), the Cauchy–Schwarz inequality, and the definition (2.10) of the energy norm. We cannot use a similar approach also for $D \in \mathcal{D}_h^{\mathrm{ext},*}$ since there is no local conservativity (3.2) on these volumes. On the other hand, however, $\varphi = 0$ on $\partial D \cap \partial\Omega$, whence

$$|(f - \nabla\cdot\mathbf{t}_h, \varphi)_D| \le \eta_{\mathrm{R},D}|||\varphi|||_D$$

for each $D \in \mathcal{D}_h^{\mathrm{ext},*}$, using the Friedrichs inequality (2.7), the Cauchy–Schwarz inequality, and the definition (2.10) of the energy norm. Finally, $|(a\nabla p_h + \mathbf{t}, \nabla\varphi)_D| \le \eta_{\mathrm{DF},D}|||\varphi|||_D$ is immediate using the fact that a is positive and scalar and the Cauchy–Schwarz inequality. Hence it now suffices to use the Cauchy–Schwarz inequality and to notice that $|||\varphi||| = 1$ in order to conclude the proof. □

The proof of following corollary is completely similar:

Corollary 3.5 (A guaranteed dual norm a posteriori error estimate)**.** *Let the assumptions of Theorem 3.4 be verified. Then*

$$|||p - p_h|||_{\#} \le \left\{\sum_{D\in\mathcal{D}_h^*} (\eta_{\mathrm{R},D} + \eta_{\mathrm{DF},D})^2\right\}^{\frac12},$$

with the diffusive flux estimator $\eta_{\mathrm{DF},D}$ *given by*

$$\eta_{\mathrm{DF},D} := \|a\nabla p_h + \mathbf{t}_h\|_D \qquad D \in \mathcal{D}_h^*, \tag{3.6}$$

and the residual estimator $\eta_{\mathrm{R},D}$ *given by*

$$\eta_{\mathrm{R},D} := m_D\|f - \nabla\cdot\mathbf{t}_h\|_D \qquad D \in \mathcal{D}_h^*, \tag{3.7}$$

where

$$m_D^2 := C_{\mathrm{P},D}h_D^2 \quad D \in \mathcal{D}_h^{\mathrm{int},*}, \qquad m_D^2 := C_{\mathrm{F},D,\partial\Omega}h_D^2 \quad D \in \mathcal{D}_h^{\mathrm{ext},*}. \tag{3.8}$$

Remark 3.6 (Assumptions of Theorem 3.4 and Corollary 3.5). Note that for Theorem 3.4 and Corollary 3.5, no additional assumptions like a polynomial form of the data, of the approximate solution, or a shape regularity of the mesh are needed.

Remark 3.7 (The mesh $\mathcal{D}_h^*$ in Theorem 3.4 or Corollary 3.5). The meshes $\mathcal{D}_h^*$ in Theorem 3.4 or Corollary 3.5 will differ in different types of estimates. Usually, either $\mathcal{D}_h^*$ is given by the dual mesh $\mathcal{D}_h$ of Section 2.1, i.e., $\mathcal{D}_h^{\mathrm{int},*} = \mathcal{D}_h^{\mathrm{int}}$ and $\mathcal{D}_h^{\mathrm{ext},*} = \mathcal{D}_h^{\mathrm{ext}}$, or $\mathcal{D}_h^{\mathrm{int},*} = \mathcal{S}_h$ and $\mathcal{D}_h^{\mathrm{ext},*} = \emptyset$ ($\mathcal{S}_h$ is given in Section 2.1), or $\mathcal{D}_h^{\mathrm{int},*} = \mathcal{T}_h$ and $\mathcal{D}_h^{\mathrm{ext},*} = \emptyset$.

Remark 3.8 (Comparison of the estimators of Theorem 3.4 and of Corollary 3.5). The estimators of Theorem 3.4 and of Corollary 3.5 coincide when $a = 1$. We find the estimators of Corollary 3.5 more physical as they measure the misfit between the true fluxes $a\nabla p_h$ and $\mathbf{t}_h$ and not their energy counterparts $a^{\frac12}\nabla p_h$ and $a^{-\frac12}\mathbf{t}_h$ in $\eta_{\mathrm{DF},D}$ and do not involve the constant $c_{a,D}$ in $\eta_{\mathrm{R},D}$.

In order to use Theorem 3.4 and Corollary 3.5 in practice, we need to construct a (finite-dimensional) $\mathbf{t}_h$ satisfying (3.2). We will look for a suitable $\mathbf{t}_h$ in the lowest-order Raviart–Thomas–Nédélec space $\mathbf{RTN}(\mathcal{S}_h)$ defined over a fine simplicial mesh $\mathcal{S}_h$ of Section 2.1 which we suppose to be a refinement of the mesh $\mathcal{D}_h^*$ from Theorem 3.4 or Corollary 3.5. The space $\mathbf{RTN}(\mathcal{S}_h) \subset \mathbf{H}(\mathrm{div},\Omega)$ is a space of vector functions having on each $K \in \mathcal{S}_h$ the form $(a_K + d_K x, b_K + d_K y)^t$ if $d = 2$ and $(a_K + d_K x, b_K + d_K y, c_K + d_K z)^t$ if $d = 3$. Note that the requirement $\mathbf{RTN}(\mathcal{S}_h) \subset \mathbf{H}(\mathrm{div},\Omega)$ imposes the continuity of the normal trace across all $\sigma \in \mathcal{G}_h^{\mathrm{int}}$ and recall that $\mathbf{v}\cdot\mathbf{n}_\sigma$ is a constant for all $\sigma \in \mathcal{G}_h$ and that these side fluxes also represent the degrees of freedom of $\mathbf{RTN}(\mathcal{S}_h)$. For more details, we refer to [16, 41]. Raviart–Thomas–Nédélec spaces have been used previously in a posteriori error estimation in a similar concept in [30, 39, 23, 32, 44, 28, 15].

3.3 Constructions of the equilibrated flux $\mathbf{t}_h$

We show here four different ways of constructing an equilibrated flux $\mathbf{t}_h$ satisfying (3.2). For this purpose, we assume from now on, on the mesh $\mathcal{D}_h$ of Section 2.1:

$$-\langle \{\!\{ a\nabla p_h \cdot \mathbf{n} \}\!\}_\omega, 1\rangle_{\partial D} = (f,1)_D \qquad \forall D \in \mathcal{D}_h^{\rm int}. \tag{3.9}$$

The weights ω are left unspecified as yet. We will see below in Section 5 that a whole collection of numerical schemes can be shown to satisfy this property.

3.3.1 Construction of $\mathbf{t}_h$ by direct prescription

We define $\mathbf{t}_h \in \mathbf{RTN}(\mathcal{S}_h)$ by

$$\mathbf{t}_h \cdot \mathbf{n}_\sigma := -\{\!\{ a\nabla p_h \cdot \mathbf{n}_\sigma \}\!\}_\omega \qquad \forall \sigma \in \mathcal{G}_h, \tag{3.10}$$

where the weights ω are the same as those in (3.9). Thus a simple (weighted) average of the normal components of the approximate flux $-a\nabla p_h$ over the sides of $\mathcal{S}_h$ is used to define the equilibrated flux $\mathbf{t}_h$. Note that by this construction, $\langle \mathbf{t}_h \cdot \mathbf{n}, 1\rangle_{\partial D} = (f,1)_D$ for all $D \in \mathcal{D}_h^{\rm int}$ is immediate, whence (3.2) follows by the Green theorem.

This construction, however, may suffer from two inconveniences. Firstly, whenever $D \in \mathcal{D}_h^{\rm int}$ is nonconvex, the Poincaré constant $C_{{\rm P},D}$ from (2.6) is no longer equal to $1/\pi^2$ and its evaluation is much more difficult leading to less sharp estimates. The second inconvenience was pointed out in [20]: as (3.2) only holds on a set of elements $\mathcal{S}_D$ and not on each $K \in \mathcal{S}_h$, the residual estimators are not higher-order terms as in [48, 24] and may dominate the diffusive flux ones. Consequently, the effectivity index does not approach the optimal value of one. The approaches of the three following sections improve on these two points (we present them in the energy norm setting, similar results in the dual norm setting are rather straightforward).

3.3.2 Construction of $\mathbf{t}_h$ by local minimization involving local linear systems solution

In [20], $\mathbf{t}_h \cdot \mathbf{n}_\sigma$ is given by (3.10) only on such $\sigma \in \mathcal{G}_h$ which are at the boundary of some $D \in \mathcal{D}_h^{\rm int}$. By the Green theorem, this is sufficient for (3.2). The remaining sides lie in the interior of some $D \in \mathcal{D}_h$ (or at the boundary of Ω), so that $\mathbf{t}_h \cdot \mathbf{n}_\sigma$ can be chosen locally and independently by local minimization of $\eta_{{\rm R},D}^2 + \eta_{{\rm DF},D}^2$ for each $D \in \mathcal{D}_h$. This leads to a solution of a small linear system for each $D \in \mathcal{D}_h$ and helps the improve the effectivity index to a value close to one.

3.3.3 Construction of $\mathbf{t}_h$ by local minimization without local linear systems solution

We suggest here an improvement of the previous approach which avoids any local systems solution.

Let $D \in \mathcal{D}_h$ be fixed. The first step is to construct $\mathbf{t}_{1,D} \in \mathbf{RTN}(\mathcal{S}_D)$ given by (3.10). In the second one, we then construct $\mathbf{t}_{2,D} \in \mathbf{RTN}(\mathcal{S}_D)$ given by (3.10) only for such $\sigma \in \mathcal{G}_h$ contained in D which are at the boundary of some $E \in \mathcal{D}_h^{\rm int}$ and such that $(\nabla\cdot\mathbf{t}_{2,D},1)_K = (f,1)_K$ for all $K \in \mathcal{S}_D$. Note that as $(\nabla \cdot \mathbf{t}_{2,D},1)_D = \langle \mathbf{t}_{2,D}\cdot\mathbf{n},1\rangle_{\partial D} = (f,1)_D$ when $D \in \mathcal{D}_h^{\rm int}$, this can be done without any (local) linear system solution by choosing the flux over one interior side and a sequential construction as $\sum_{K\in\mathcal{S}_D}(f,1)_K = (f,1)_D$. If $D \in \mathcal{D}_h^{\rm ext}$, this argument is then replaced by the fact that we are free to choose the fluxes over the exterior sides. Now any $\mathbf{t}_D := \alpha\mathbf{t}_{1,D} + (1-\alpha)\mathbf{t}_{2,D}$ obviously obeys (3.2) and we can minimize $\eta_D := \eta_{{\rm R},D} + \eta_{{\rm DF},D}$ as a function of the parameter α. It turns out that it is much easier to minimize $\eta_{{\rm R},D}^2 + \eta_{{\rm DF},D}^2$, as this is a quadratic function of α,

and the optimal value is easily found to be given by

$$\begin{aligned} & \alpha\big(\|a^{-\frac12}(\mathbf{t}_{1,D}-\mathbf{t}_{2,D})\|_D^2 + m_{D,a}^2\|\nabla\cdot(\mathbf{t}_{1,D}-\mathbf{t}_{2,D})\|_D^2\big) \\ = \quad & -(a^{\frac12}\nabla p_h + a^{-\frac12}\mathbf{t}_{2,D}, a^{-\frac12}(\mathbf{t}_{1,D}-\mathbf{t}_{2,D}))_D \\ & +m_{D,a}^2(f-\nabla\cdot\mathbf{t}_{2,D}, \nabla\cdot(\mathbf{t}_{1,D}-\mathbf{t}_{2,D}))_D. \end{aligned}$$

As however this value does not necessarily minimize η_D (when it is uniquely defined by the above formula) but $\eta_{\mathrm{R},D}^2+\eta_{\mathrm{DF},D}^2$, we finally propose as an improved estimator

$$\eta_D := \min\{\eta_D(\mathbf{t}_{1,D}), \eta_D(\mathbf{t}_{2,D}), \eta_D(\alpha\mathbf{t}_{1,D}+(1-\alpha)\mathbf{t}_{2,D})\}. \tag{3.11}$$

Such an estimator will be locally efficient (and robust) whenever it is the case for $\eta_D(\mathbf{t}_{1,D})$.

3.3.4 Construction of $\mathbf{t}_h$ by mixed finite element approximations of local Neumann/Dirichlet problems

We adapt here to the present setting the approach of [25]. In context of a posteriori error estimation, solution of local Neumann problems can be traced back at least to [10].

For a given $D\in\mathcal{D}_h$, let

$$\mathbf{RTN}_{\mathrm{N}}(\mathcal{S}_D) := \{\mathbf{v}_h\in\mathbf{RTN}(\mathcal{S}_D);\ \mathbf{v}_h\cdot\mathbf{n}_\sigma = -a\nabla p_h\cdot\mathbf{n}_\sigma \quad \forall\sigma\in\mathcal{G}_h^{\mathrm{int}}\cap\partial D\}.$$

We suppose here that a is piecewise constant on $\mathcal{T}_h$ (in this case, in particular, the choice of the weights ω in (3.9) has no influence). Let f_h be given by $(f,1)_K/|K|$ for all $K\in\mathcal{S}_h$. We then define $\mathbf{t}_h\in\mathbf{RTN}(\mathcal{S}_h)$ by solving on each $D\in\mathcal{D}_h$ the following minimization problem:

$$\mathbf{t}_h|_D := \arg\inf_{\mathbf{v}_h\in\mathbf{RTN}_{\mathrm{N}}(\mathcal{S}_D),\,\nabla\cdot\mathbf{v}_h=f_h} \|a^{\frac12}\nabla p_h + a^{-\frac12}\mathbf{v}_h\|_D. \tag{3.12}$$

Define $\mathbf{RTN}_{\mathrm{N},0}(\mathcal{S}_D)$ as $\mathbf{RTN}_{\mathrm{N}}(\mathcal{S}_D)$ but with the normal flux condition $\mathbf{v}_h\cdot\mathbf{n}_\sigma=0$. Let $\mathbb{P}_0^*(\mathcal{S}_D)$ be spanned by piecewise constants on $\mathcal{S}_D$ with zero mean on D when $D\in\mathcal{D}_h^{\mathrm{int}}$; when $D\in\mathcal{D}_h^{\mathrm{ext}}$, the mean value condition is not imposed. Then it is easy to show that (3.12) is equivalent to finding $\mathbf{t}_h\in\mathbf{RTN}_{\mathrm{N}}(\mathcal{S}_D)$ and $q_h\in\mathbb{P}_0^*(\mathcal{S}_D)$, the mixed finite element approximations of local Neumann problems on $D\in\mathcal{D}_h^{\mathrm{int}}$ and local Neumann/Dirichlet problems on $D\in\mathcal{D}_h^{\mathrm{ext}}$:

$$(a^{-1}\mathbf{t}_h+\nabla p_h, \mathbf{v}_h)_D - (q_h, \nabla\cdot\mathbf{v}_h)_D = 0 \qquad \forall\mathbf{v}_h\in\mathbf{RTN}_{\mathrm{N},0}(\mathcal{S}_D), \tag{3.13a}$$

$$(\nabla\cdot\mathbf{t}_h, \phi_h)_D = (f,\phi_h)_D \qquad \forall\phi_h\in\mathbb{P}_0^*(\mathcal{S}_D). \tag{3.13b}$$

Note in particular that the function $-a\nabla p_h\cdot\mathbf{n}_\sigma$ on the boundary of each $D\in\mathcal{D}_h^{\mathrm{int}}$ by (3.9) satisfies the Neumann compatibility condition, whence also the existence and uniqueness follow. Theorem 3.4 and Corollary 3.5 can be used here with $\mathcal{D}_h^{\mathrm{int},*}=\mathcal{S}_h$ and $\mathcal{D}_h^{\mathrm{ext},*}=\emptyset$. The above presentation is done in the energy norm (2.10) setting. For the dual norm (2.11), we merely need to replace $(a^{-1}\mathbf{t}_h+\nabla p_h,\mathbf{v}_h)_D$ by $(\mathbf{t}_h+a\nabla p_h,\mathbf{v}_h)_D$ in (3.13a). A solution of a local linear system on each $D\in\mathcal{D}_h$ is necessary in this approach but the results of Section 6 below reveal excellent.

3.4 Remarks and generalizations

Remark 3.9 (Comparison with standard residual estimators). The above estimates have three basic advantages in comparison with standard residual estimators, cf. Verfürth [45]. First of all, they feature no undetermined constant and deliver a guaranteed upper bound. Next, the classical residual estimator $h_K\|f\|_K$ is replaced by its improved version (3.4). Lastly, as it will be seen in Section 4 below, our estimates represent local lower bounds for the classical residual estimators. The improved behavior of our estimators over the classical one for the finite element method is numerically studied in [20].

Remark 3.10 (Comparison with the equilibrated residual method). In the equilibrated residual method, cf. [3], one searches equilibrated side fluxes expressing local conservativity over each $K \in \mathcal{T}_h$, by means of solution of local linear systems. Contrarily to this approach, our estimators are based on the immediately available conservativity of the finite element method over the dual grids $\mathcal{D}_h$ (see Remark 5.13 below). On the other hand, we suggest the present approach only for lowest-order finite elements, whereas the approach of [3] works for any order. Remark that a guaranteed and locally computable upper bound can also be obtained in the equilibrated residual method if the data oscillation term is separated as in [2].

Remark 3.11 (Comparison with the Zienkiewicz–Zhu averaging). Similarly as in the Zienkiewicz–Zhu [52] estimator, we look here for a smoothened (averaged) flux $\mathbf{t}_h$. We, however, only impose $\mathbf{t}_h \in \mathbf{H}(\mathrm{div}, \Omega)$, i.e., only the normal component and not the whole vector field continuity. Also, the present residual estimators $\eta_{\mathrm{R},D}$ can become crucial on rough meshes or in the presence of the material coefficient a, see also the discussion in [27].

Remark 3.12 (Comparison with functional a posteriori estimates). Repin [39] or Korotov [28] use instead of Theorem 3.4 the estimate

$$|||p - p_h||| \le \frac{C_{\mathrm{F},\Omega}^{1/2} h_\Omega}{c_{a,\Omega}^{1/2}} \|f - \nabla \cdot \mathbf{t}_h\| + \|a^{\frac{1}{2}} \nabla p_h + a^{-\frac{1}{2}} \mathbf{t}_h\|,$$

which follows readily from Theorem 3.1 using the Cauchy–Schwarz inequality, the Friedrichs inequality, and the definition of the energy seminorm. Here p is the weak solution given by (2.9), $p_h \in H_0^1(\Omega)$ and $\mathbf{t}_h \in \mathbf{H}(\mathrm{div}, \Omega)$ are arbitrary, $C_{\mathrm{F},\Omega}$ is the constant from the Friedrichs inequality (2.7) with $D = \Omega$, and h_Ω is the diameter of Ω. The advantage is that no particular construction of $\mathbf{t}_h \in \mathbf{H}(\mathrm{div}, \Omega)$ has to be done and the estimate is thus fully scheme-independent. However, as no information from the computation is used, the residual term is in general too large by the presence of h_Ω instead of h_D which we find in Theorem 3.4. Secondly, the term $1/c_{a,\Omega}^{1/2}$ is also greatly unfavorable in comparison with $1/c_{a,D}^{1/2}$ found in our estimates. Thus, a rather expensive global minimization is usually employed in the type of estimates of [39] or [28].

Remark 3.13 (Comparison with the estimator of Luce and Wohlmuth [32]). Our estimators are close to those of Luce and Wohlmuth [32], in particular in that we construct the dual mesh $\mathcal{D}_h$ and the second simplicial triangulation $\mathcal{S}_h$ and a $\mathbf{t}_h \in \mathbf{RTN}(\mathcal{S}_h)$. One particular point is that the construction of $\mathbf{t}_h$ by (3.10) with harmonic averaging, as shown in Section 4.1 below, leads to full robustness with respect to discontinuous coefficients in the energy norm.

Remark 3.14 (Residual estimators and data oscillation). Note that whenever $f \in H^1(K)$ for all $K \in \mathcal{S}_h$, the residual estimators $\eta_{\mathrm{R},D}$ in Section 3.3.4 (or those of Section 3.3.3 with $\mathbf{t}_{2,D}$ only) represent a contribution of higher order, as $\|f - f_h\|_K \le 1/\pi h_K \|\nabla f\|_K$ by the Poincaré inequality (2.6) (using the convexity of simplices). Moreover, if f is piecewise constant on $\mathcal{S}_h$, they disappear completely.

4 Efficiency and robustness of the a posteriori error estimates

We prove here the (local) efficiency and robustness of our estimates. We first present a robustness energy norm result in case of discontinuities aligned with the dual meshes and use of harmonic averaging. Then robustness in the dual norm without any special requirement is proven. Finally, some generalizations are discussed.

4.1 Local efficiency and robustness of the energy norm estimate for harmonic weighting and dual mesh-aligned discontinuities

The result of this section is given in the energy norm (2.10) and only applies to the case where a is piecewise constant on $\mathcal{D}_h$ and ω in (3.9) represents harmonic weighting.

Theorem 4.1 (Local efficiency and robustness of the energy norm estimate for harmonic weighting and dual mesh-aligned discontinuities)**.** *Let a be piecewise constant on $\mathcal{D}_h$, let f be a piecewise polynomial of degree m on $\mathcal{S}_h$, let p be the weak solution of problem (1.1a)–(1.1b), and let $p_h \in X_h^0$ satisfy (3.9) with the weights (2.5). Let next $\mathcal{S}_h$ be shape-regular with the constant $\kappa_{\mathcal{S}}$ and let $\mathbf{t}_h$ be given by (3.10), $\eta_{\mathrm{DF},D}$ given by (3.3), and $\eta_{\mathrm{R},D}$ by (3.4), $\mathcal{D}_h^* = \mathcal{D}_h$ in Theorem 3.4. Then, for each $D \in \mathcal{D}_h$, there holds*

$$\eta_{\mathrm{DF},D} \le C|||p - p_h|||_{\mathcal{T}_{V_D}}, \tag{4.1a}$$

$$\eta_{\mathrm{R},D} \le \tilde{C}|||p - p_h|||_{\mathcal{T}_{V_D}}, \tag{4.1b}$$

where the constant C depends only on d, $\kappa_{\mathcal{S}}$, and m and $\tilde{C}$ in addition depends on $C_{\mathrm{P},D}$ if $D \in \mathcal{D}_h^{\mathrm{int}}$ or $C_{\mathrm{F},D,\partial\Omega}$ if $D \in \mathcal{D}_h^{\mathrm{ext}}$.

The proof of Theorem 4.1 is decomposed into two parts. For $\eta_{\mathrm{DF},D}$, Lemma 4.2 shows that the construction (3.10) implies that the normal components of $\mathbf{t}_h$ differ from those of $a\nabla p_h$ by the jumps of $a\nabla p_h \cdot \mathbf{n}$. The latter are a part of residual estimators and are therefore known to be bounded by the error. The second estimator, $\eta_{\mathrm{R},D}$, is then efficient due to a complementarity argument as shown in Lemma 4.3.

Lemma 4.2 (Local efficiency of the diffusive flux estimator)**.** *Let the assumptions of Theorem 4.1 be verified. Then (4.1a) holds true.*

Proof. The proof follows the techniques of [45] and [24]. Recall first the standard estimate

$$\|\mathbf{v}_h\|_K^2 \le Ch_K \sum_{\sigma\in\mathcal{E}_K} \|\mathbf{v}_h \cdot \mathbf{n}\|_\sigma^2 \tag{4.2}$$

valid for each $\mathbf{v}_h \in \mathbf{RTN}(K)$ and any simplex K. Here, and similarly in the rest of the proof, the constant C, not necessarily the same at each occurrence, depends only on d, $\kappa_{\mathcal{S}}$, and m.

Let now K be an arbitrary element in the simplicial mesh $\mathcal{S}_D$ of a given $D \in \mathcal{D}_h$ and let us put $\mathbf{v}_h = a\nabla p_h + \mathbf{t}_h$. We have

$$\|a^{\frac12}\nabla p_h + a^{-\frac12}\mathbf{t}_h\|_K^2 = a_K^{-1}\|\mathbf{v}_h\|_K^2 \le Ca_K^{-1}h_K \sum_{\sigma\in\mathcal{E}_K\cap\mathcal{G}_h^{\mathrm{int}}} \|\omega_{L,\sigma}[\![a\nabla p_h \cdot \mathbf{n}_\sigma]\!]\|_\sigma^2, \tag{4.3}$$

where L denotes the neighboring element to K across $\sigma \in \mathcal{G}_h^{\mathrm{int}}$, using that

$$(a\nabla p_h + \mathbf{t}_h)|_K \cdot \mathbf{n}_\sigma = (a\nabla p_h \cdot \mathbf{n}_\sigma)|_K - \{\!\{a\nabla p_h \cdot \mathbf{n}_\sigma\}\!\}_\omega = \mathbf{n}_\sigma \cdot \mathbf{n}\, \omega_{L,\sigma}[\![a\nabla p_h \cdot \mathbf{n}_\sigma]\!] \tag{4.4}$$

for $\sigma \in \mathcal{E}_K \cap \mathcal{G}_h^{\mathrm{int}}$ and $(a\nabla p_h + \mathbf{t}_h)|_K \cdot \mathbf{n}_\sigma = 0$ for $\sigma \in \mathcal{E}_K \cap \mathcal{G}_h^{\mathrm{ext}}$. Note that $\mathbf{n}_\sigma \cdot \mathbf{n} = \pm 1$ is only used as a sign determination.

Let us now consider a fixed $\sigma = \sigma_{K,L} \in \mathcal{E}_K \cap \mathcal{G}_h^{\mathrm{int}}$. The estimate

$$h_K^{\frac12}\|[\![a\nabla p_h \cdot \mathbf{n}_\sigma]\!]\|_\sigma \le C \sum_{M\in\{K,L\}} a_M^{\frac12}|||p - p_h|||_M.$$

is standard using the side and element bubble functions, the Green theorem, the inverse inequality, and the equivalence of norms on finite-dimensional spaces, cf. [45]. It then follows that

$$\omega_{L,\sigma} a_K^{-\frac{1}{2}} h_K^{\frac{1}{2}} \|[\![a\nabla p_h \cdot \mathbf{n}_\sigma]\!]\|_\sigma \le C \sum_{M\in\{K,L\}} \omega_{L,\sigma} a_K^{-\frac{1}{2}} a_M^{\frac{1}{2}} |||p - p_h|||_M.$$

Finally, thanks to the definition (2.2) of $\omega_{L,\sigma}$, $\omega_{L,\sigma} a_K^{-\frac{1}{2}} a_M^{\frac{1}{2}} = \omega_{L,\sigma} \le 1$ if $M = K$ and by (2.5), $\omega_{L,\sigma} a_K^{-\frac{1}{2}} a_M^{\frac{1}{2}} = a_K (a_K + a_L)^{-1} a_K^{-\frac{1}{2}} a_L^{\frac{1}{2}} \le \frac{1}{2}$ if $M = L$, using the inequality $2ab \le a^2 + b^2$.

Now finally, using the above results,

$$\begin{aligned}
\eta_{\mathrm{DF},D}^2 &= \sum_{K\in\mathcal{S}_D} \|a^{\frac{1}{2}}\nabla p_h + a^{-\frac{1}{2}}\mathbf{t}_h\|_K^2 \\
&\le C \sum_{K\in\mathcal{S}_D} \sum_{\sigma_{K,L}\in\mathcal{E}_K\cap\mathcal{G}_h^{\mathrm{int}}} a_K^{-1} h_K \omega_{L,\sigma_{K,L}}^2 \|[\![a\nabla p_h \cdot \mathbf{n}_{\sigma_{K,L}}]\!]\|_{\sigma_{K,L}}^2 \\
&\le C \sum_{K\in\mathcal{S}_D} \sum_{\sigma_{K,L}\in\mathcal{E}_K\cap\mathcal{G}_h^{\mathrm{int}}} \sum_{M\in\{K,L\}} |||p - p_h|||_M^2 \le C |||p - p_h|||_{\mathcal{T}_{V_D}}^2,
\end{aligned}$$

which was to be proved. □

Lemma 4.3 (Local efficiency of the residual estimator)**.** *Let the assumptions of Theorem 4.1 be verified. Then* (4.1b) *holds true.*

Proof. Let us consider a fixed $D \in \mathcal{D}_h$. First,

$$\|f - \nabla\cdot\mathbf{t}_h\|_K \le C a_K^{\frac{1}{2}} h_K^{-1} \|a^{\frac{1}{2}}\nabla p + a^{-\frac{1}{2}}\mathbf{t}_h\|_K$$

for each $K \in \mathcal{S}_D$ with C depending only on d, $\kappa_{\mathcal{S}}$, and m follows standardly by using the element bubble function, the equivalence of norms on finite-dimensional spaces, definition (2.9) of the weak solution, the Green theorem, the Cauchy–Schwarz inequality, definition (2.10) of the energy norm, and the inverse inequality, cf. [45] or [48, Lemma 7.6]. Hence

$$\|f - \nabla\cdot\mathbf{t}_h\|_D \le C C_{a,D}^{\frac{1}{2}} h_D^{-1} \|a^{\frac{1}{2}}\nabla p + a^{-\frac{1}{2}}\mathbf{t}_h\|_D$$

holds true, using also the fact that $h_D / \min_{K\in\mathcal{S}_D} h_K$ is bounded by the shape-regularity of $\mathcal{S}_h$. Thus

$$h_D c_{a,D}^{-\frac{1}{2}} \|f - \nabla\cdot\mathbf{t}_h\|_D \le C c_{a,D}^{-\frac{1}{2}} C_{a,D}^{\frac{1}{2}} \|a^{\frac{1}{2}}\nabla p + a^{-\frac{1}{2}}\mathbf{t}_h\|_D.$$

Next note that $c_{a,D}^{-\frac{1}{2}} C_{a,D}^{\frac{1}{2}} = 1$ for a piecewise constant on $\mathcal{D}_h$. Finally,

$$\|a^{\frac{1}{2}}\nabla p + a^{-\frac{1}{2}}\mathbf{t}_h\|_D \le |||p - p_h|||_D + \|a^{\frac{1}{2}}\nabla p_h + a^{-\frac{1}{2}}\mathbf{t}_h\|_D$$

using the triangle inequality, which concludes the proof by virtue of the previously proved estimate (4.1a). □

4.2 Global efficiency and robustness of the dual norm a posteriori error estimates

The result of this section is given in the dual norm (2.11) and applies without any restriction on the distribution of discontinuities or type of averaging in (3.9).

Theorem 4.4 (Global efficiency and robustness of the dual norm a posteriori error estimates)**.** *Let f be a piecewise polynomial of degree m on $\mathcal{S}_h$, let p be the weak solution of problem (1.1a)–(1.1b), and let $p_h \in X_h^0$ satisfy (3.9) with any weights satisfying (2.2). Let next $\mathcal{S}_h$ be shape-regular with the constant $\kappa_{\mathcal{S}}$ and let $\mathbf{t}_h$ be given by (3.10), $\eta_{\mathrm{DF},D}$ by (3.6), and $\eta_{\mathrm{R},D}$ by (3.7), $\mathcal{D}_h^* = \mathcal{D}_h$ in Corollary 3.5. Then, there holds*

$$\left\{\sum_{D\in\mathcal{D}_h}(\eta_{\mathrm{DF},D}+\eta_{\mathrm{R},D})^2\right\}^{\frac12} \le C|||p-p_h|||_{\#}, \tag{4.5}$$

where the constant C depends only on d, $\kappa_{\mathcal{S}}$, m, and $C_{\mathrm{P},D}$ for $D\in\mathcal{D}_h^{\mathrm{int}}$ and $C_{\mathrm{F},D,\partial\Omega}$ for $D\in\mathcal{D}_h^{\mathrm{ext}}$.

Proof. Throughout this proof, C denotes a generic constant with the dependencies indicated in the announcement, possibly different at different occurrences. Let $K\in\mathcal{S}_D$, $D\in\mathcal{D}_h$ be given. Adding and subtracting $\nabla\cdot(a\nabla p_h)$, using the triangle inequality, the fact that $h_D\le Ch_K$, and the inverse inequality, we have

$$\begin{aligned}C_{\mathrm{P},D}^{\frac12}h_D\|f-\nabla\cdot\mathbf{t}_h\|_K &\le C_{\mathrm{P},D}^{\frac12}h_D(\|f+\nabla\cdot(a\nabla p_h)\|_K+\|\nabla\cdot(a\nabla p_h+\mathbf{t}_h)\|_K)\\ &\le Ch_K\|f+\nabla\cdot(a\nabla p_h)\|_K+C\|a\nabla p_h+\mathbf{t}_h\|_K.\end{aligned}$$

Using (4.2), (3.10), (4.4), and (2.2), we obtain

$$\|a\nabla p_h+\mathbf{t}_h\|_K^2 \le Ch_K\sum_{\sigma\in\mathcal{E}_K\cap\mathcal{G}_h^{\mathrm{int}}}\|[\![a\nabla p_h\cdot\mathbf{n}_\sigma]\!]\|_\sigma^2$$

(note that in both cases that a is piecewise constant on $\mathcal{T}_h$ or that a is piecewise constant on $\mathcal{D}_h$, a is piecewise constant on $\mathcal{S}_h$). Combining the two above estimates,

$$\sum_{D\in\mathcal{D}_h}(\eta_{\mathrm{DF},D}+\eta_{\mathrm{R},D})^2 \le C\left(\sum_{K\in\mathcal{S}_h}h_K^2\|f+\nabla\cdot(a\nabla p_h)\|_K^2+\sum_{\sigma\in\mathcal{G}_h^{\mathrm{int}}}h_\sigma\|[\![a\nabla p_h\cdot\mathbf{n}_\sigma]\!]\|_\sigma^2\right).$$

Note that this means that the present estimates represent a lower bound for the standard residual ones (cf. [45]). The rest of the proof is based on the tools from [46].

We next prove that

$$\left\{\sum_{K\in\mathcal{S}_h}h_K^2\|f+\nabla\cdot(a\nabla p_h)\|_K^2\right\}^{\frac12} \le C|||p-p_h|||_{\#}. \tag{4.6}$$

Let $K\in\mathcal{S}_h$. Denote by ψ_K the element bubble function (cf. [45]) and put $v_K := (f+\nabla\cdot(a\nabla p_h))|_K$. By the equivalence of norms on finite-dimensional spaces, properties of the bubble functions, and definition (2.9) of the weak solution, we have, cf. [45],

$$\|v_K\|_K^2 \le C(a\nabla(p-p_h),\nabla(\psi_K v_K))_K.$$

Next, by the inverse inequality and the properties of the bubble functions,

$$h_K^2\|\nabla(\psi_K v_K)\|_K \le Ch_K\|v_K\|_K.$$

Put $\lambda|_K = h_K^2 \psi_K v_K$ and note that $\lambda \in H_0^1(\Omega)$. Using the two above inequalities,

$$\sum_{K\in\mathcal{S}_h} h_K^2 \|v_K\|_K^2 \le C \sum_{K\in\mathcal{S}_h} h_K^2 (a\nabla(p-p_h), \nabla(\psi_K v_K))_K = C \frac{\mathcal{B}(p-p_h,\lambda)}{\|\nabla\lambda\|} \|\nabla\lambda\|$$
$$\le C|||p-p_h|||_\# \left\{ \sum_{K\in\mathcal{S}_h} h_K^4 \|\nabla(\psi_K v_K)\|_K^2 \right\}^{\frac12} \le C|||p-p_h|||_\# \left\{ \sum_{K\in\mathcal{S}_h} h_K^2 \|v_K\|_K^2 \right\}^{\frac12}$$

employing also the definition (2.11) of the dual norm and the Cauchy–Schwarz inequality. Thus (4.6) is proved.

The final point of the proof is to show that

$$\left\{ \sum_{\sigma\in\mathcal{G}_h^{\rm int}} h_\sigma \|[\![a\nabla p_h \cdot \mathbf{n}_\sigma]\!]\|_\sigma^2 \right\}^{\frac12} \le C|||p-p_h|||_\#. \tag{4.7}$$

For $\sigma \in \mathcal{G}_h^{\rm int}$, put $v|_\sigma := [\![a\nabla p_h \cdot \mathbf{n}_\sigma]\!]$; we keep the same notation for the lifting of $v|_\sigma$ to the two simplices K and L sharing the side σ. Let ψ_σ be the face bubble function (cf. once again [45]). Then there holds

$$\|v_\sigma\|_\sigma^2 \le C\langle v_\sigma, \psi_\sigma v_\sigma\rangle_\sigma,$$
$$\|\psi_\sigma v_\sigma\|_K \le C h_\sigma^{\frac12} \|v_\sigma\|_\sigma.$$

Put $\lambda := \sum_{\sigma\in\mathcal{G}_h^{\rm int}} h_\sigma \psi_\sigma v_\sigma$. Note that $\lambda \in H_0^1(\Omega)$, as only the interior sides appear in the sum. Finally, note that by the second of the above inequalities,

$$\|\lambda\|_K \le \sum_{\sigma\in\mathcal{E}_K\cap\mathcal{G}_h^{\rm int}} h_\sigma \|\psi_\sigma v_\sigma\|_K \le C \sum_{\sigma\in\mathcal{E}_K\cap\mathcal{G}_h^{\rm int}} h_\sigma^{\frac32} \|v_\sigma\|_\sigma.$$

Using the above inequalities and the Green theorem,

$$\sum_{\sigma\in\mathcal{G}_h^{\rm int}} h_\sigma \|v_\sigma\|_\sigma^2$$
$$\le C \sum_{\sigma\in\mathcal{G}_h^{\rm int}} \langle [\![a\nabla p_h \cdot \mathbf{n}_\sigma]\!], \lambda\rangle_\sigma = C \sum_{K\in\mathcal{S}_h} \{(f + \nabla\cdot(a\nabla p_h), \lambda)_K - (a\nabla(p-p_h), \nabla\lambda)_K\}$$
$$\le C|||p-p_h|||_\# \|\nabla\lambda\| + C \left\{ \sum_{K\in\mathcal{S}_h} h_K^2 \|f + \nabla\cdot(a\nabla p_h)\|_K^2 \right\}^{\frac12} \left\{ \sum_{K\in\mathcal{S}_h} h_K^{-2} \|\lambda\|_K^2 \right\}^{\frac12}$$
$$\le C|||p-p_h|||_\# \left\{ \sum_{K\in\mathcal{S}_h} h_K^{-2} \|\lambda\|_K^2 \right\}^{\frac12} \le C|||p-p_h|||_\# \left\{ \sum_{\sigma\in\mathcal{G}_h^{\rm int}} h_\sigma \|v_\sigma\|_\sigma^2 \right\}^{\frac12},$$

where we have also employed (4.6), the inverse inequality, and the Cauchy–Schwarz inequality. Thus (4.7) is proved. □

4.3 Efficiency of the estimates by local Neumann/Dirichlet problems

We show here the efficiency of the estimates constructed using the approach of Section 3.3.4. For simplicity, we present the result in the energy norm (2.10) setting only; a similar (robust) result

in the dual norm (2.11) can likewise be established. We only show here that our estimates in this case represent local lower bounds for the classical residual ones; local efficiency proof can the be completed using the standard results, cf. [45] or Sections 4.1 and 4.2.

Theorem 4.5 (Efficiency of the estimates by local Neumann/Dirichlet problems)**.** *Let the assumptions of Section 3.3.4 be verified, let* $\mathbf{t}_h$ *be the solution of* (3.13a)–(3.13b)*, let* $\mathcal{S}_h$ *be shape-regular with the constant* $\kappa_{\mathcal{S}}$*, and consider the energy norm* (2.10) *setting and* $\mathcal{D}_h^{\mathrm{int},*} = \mathcal{S}_h$ *and* $\mathcal{D}_h^{\mathrm{ext},*} = \emptyset$ *in Theorem 3.4. Then, for all* $D \in \mathcal{D}_h$*,*

$$\eta_{\mathrm{R},K} = C_{\mathrm{P},K}^{\frac{1}{2}} \frac{h_K}{c_{a,K}^{\frac{1}{2}}} \|f - f_h\|_K \qquad \forall K \in \mathcal{S}_D, \tag{4.8}$$

$$\left\{ \sum_{K \in \mathcal{S}_D} \eta_{\mathrm{DF},K}^2 \right\}^{\frac{1}{2}} \leq C c_{a,D}^{-\frac{1}{2}} \left(\left\{ \sum_{K \in \mathcal{S}_D} h_K^2 \|f_h + \nabla \cdot (a \nabla p_h)\|_K^2 \right\}^{\frac{1}{2}} + \left\{ \sum_{\sigma \in \mathcal{G}_D^{\mathrm{int}}} h_\sigma \|[\![a \nabla p_h \cdot \mathbf{n}_\sigma]\!]\|_\sigma^2 \right\}^{\frac{1}{2}} \right), \tag{4.9}$$

where the constant C *depends only on* d *and* $\kappa_{\mathcal{S}}$*.*

Proof. Firstly, (4.8) is an immediate consequence of (3.13b). Let $D \in \mathcal{D}_h$ be fixed. To show (4.9), we first need a hybridized version of (3.13a)–(3.13b), cf. [16, 41]. Therein, (3.13a) is replaced by

$$(a^{-1}\mathbf{t}_h + \nabla p_h, \mathbf{v}_h)_D - (q_h, \nabla \cdot \mathbf{v}_h)_D + \sum_{K \in \mathcal{S}_D} \langle \mathbf{v}_h \cdot \mathbf{n}, \lambda_h \rangle_{\partial K} = 0 \qquad \forall \mathbf{v}_h \in \mathbf{RTN}_{\mathrm{N},0}^*(\mathcal{S}_D);$$

$\mathbf{RTN}_{\mathrm{N},0}^*(\mathcal{S}_D)$ is the same space as $\mathbf{RTN}_{\mathrm{N},0}(\mathcal{S}_D)$ with, however, no normal trace continuity constraint and λ_h is the Lagrange multiplier. In this hybridized version, we can put $\mathbf{v}_h = \mathbf{t}_h + a\nabla p_h$ to infer that

$$\|a^{\frac{1}{2}} \nabla p_h + a^{-\frac{1}{2}} \mathbf{t}_h\|_D^2 = (q_h, f_h + \nabla \cdot (a \nabla p_h))_D - \sum_{\sigma \in \mathcal{G}_D^{\mathrm{int}}} \langle [\![a \nabla p_h \cdot \mathbf{n}]\!], \lambda_h \rangle_\sigma, \tag{4.10}$$

using that $\nabla \cdot \mathbf{t}_h = f_h$ by (3.13b) and that the normal trace of $\mathbf{t}_h$ is continuous. Next, employing the approach of [48, Section 4.1] (cf. also [6, 5]), there exists a postprocessing $\tilde{q}_h \in M(\mathcal{S}_D)$ of q_h such that

$$-a\nabla \tilde{q}_h = \mathbf{t}_h + a\nabla p_h \qquad \forall K \in \mathcal{S}_D, \tag{4.11a}$$

$$(\tilde{q}_h, 1)_K = q_h|_K |K| \qquad \forall K \in \mathcal{S}_D, \tag{4.11b}$$

$$\langle \tilde{q}_h, 1 \rangle_\sigma = \lambda_h|_\sigma |\sigma| \qquad \forall \sigma \in \mathcal{G}_D^{\mathrm{int}}, \tag{4.11c}$$

$$\langle \tilde{q}_h, 1 \rangle_\sigma = 0 \qquad \forall \sigma \in \mathcal{G}_D^{\mathrm{ext}} \subset \partial\Omega. \tag{4.11d}$$

Here, $M(\mathcal{S}_D)$ is a space of particular piecewise polynomials on $\mathcal{S}_D$ of total degree ≤ 2. Let hereafter C be a generic constant only dependent on d and $\kappa_{\mathcal{S}}$, possibly different at different occurrences. Note that the mean value of $\tilde{q}_h$ over D is zero when $D \in \mathcal{D}_h^{\mathrm{int}}$, whereas mean values over the sides lying in $\partial\Omega$ are zero when $D \in \mathcal{D}_h^{\mathrm{ext}}$. Thus, for both $D \in \mathcal{D}_h^{\mathrm{int}}$ and $D \in \mathcal{D}_h^{\mathrm{ext}}$, we have the Poincaré/Friedrichs inequality $\|\tilde{q}_h\| \leq C h_D \|\nabla \tilde{q}_h\|_D$, cf. [47]. Employing also the inverse inequality $\|\tilde{q}_h\|_\sigma \leq C h_\sigma^{-\frac{1}{2}} \|\tilde{q}_h\|_K$ for any K sharing $\sigma \in \mathcal{G}_D^{\mathrm{int}}$, the Cauchy–Schwarz inequality, and the facts that $h_D / \min_{K \in \mathcal{S}_D} h_K$ and the number of elements in $\mathcal{S}_D$ are bounded by the shape-regularity of

$\mathcal{S}_h$, we infer from (4.10)

$$\begin{aligned}
&\|a^{\frac12}\nabla p_h + a^{-\frac12}\mathbf{t}_h\|_D^2\\
=&(\tilde q_h, f_h + \nabla\cdot(a\nabla p_h))_D - \sum_{\sigma\in\mathcal{G}_D^{\rm int}} \langle [\![a\nabla p_h\cdot\mathbf{n}]\!], \tilde q_h\rangle_\sigma\\
\le&\|\tilde q_h\|_D \|f_h + \nabla\cdot(a\nabla p_h)\|_D + C\left\{\sum_{\sigma\in\mathcal{G}_D^{\rm int}} h_\sigma^{-1}\|[\![a\nabla p_h\cdot\mathbf{n}_\sigma]\!]\|_\sigma^2\right\}^{\frac12}\|\tilde q_h\|_D\\
\le&C\|\nabla\tilde q_h\|_D\left(\left\{\sum_{K\in\mathcal{S}_D} h_K^2\|f_h+\nabla\cdot(a\nabla p_h)\|_K^2\right\}^{\frac12} + \left\{\sum_{\sigma\in\mathcal{G}_D^{\rm int}} h_\sigma\|[\![a\nabla p_h\cdot\mathbf{n}_\sigma]\!]\|_\sigma^2\right\}^{\frac12}\right).
\end{aligned}$$

The assertion follows from (4.11a) while scaling by $c_{a,D}^{-\frac12}$ and dividing by $\|a^{\frac12}\nabla p_h + a^{-\frac12}\mathbf{t}_h\|_D$. □

4.4 Remarks and generalizations

We conclude this section by several remarks and comments on generalizations.

Remark 4.6 (Unconditioned energy norm robustness with respect to discontinuous a). When a is piecewise constant on $\mathcal{D}_h$ and when the harmonic averaging (2.5) has been used, equations (4.1a)–(4.1b) imply a full robustness of the estimators of Theorem 3.4 with respect to the diffusion coefficient a. No condition on the spatial distribution of the discontinuities in a is necessary, whereas in the previous results [12, 35, 22, 1, 17], a "monotonicity around vertices" condition or a similar assumption on the distribution of the diffusion coefficient was always necessary.

Remark 4.7 (Diffusion coefficient a piecewise constant on $\mathcal{T}_h$). If a is piecewise constant on $\mathcal{T}_h$ (whence the choice of the weights has no influence in (3.9)) but harmonic averaging (2.5) has been used in order to define the diffusive flux $\mathbf{t}_h$ in (3.10), equation (4.1a) still holds true, i.e., the diffusive flux estimator $\eta_{{\rm DF},D}$ is still fully robust. It however follows from the proof of Lemma 4.3 that in equation (4.1b), an additional factor $c_{a,D}^{-\frac12}C_{a,D}^{\frac12}$ appears, whence the residual estimator $\eta_{{\rm R},D}$ is not robust in this case. Note also that as $-a\nabla p_h\cdot\mathbf{n}_\sigma = \mathbf{t}_h\cdot\mathbf{n}_\sigma$ for all $\sigma\subset\partial D$ in this case, one here actually comes to

$$\begin{aligned}
\eta_{{\rm DF},D} &\le C|||p-p_h|||_D,\\
\eta_{{\rm R},D} &\le \tilde C|||p-p_h|||_D,
\end{aligned}$$

i.e., one has the local efficiency directly on each dual volume $D\in\mathcal{D}_h$ and not on the patch $\mathcal{T}_{V_D}$ of the original simplicial elements sharing the vertex V_D.

Remark 4.8 (Unconditioned dual norm robustness). Note that Theorem 4.4 gives full robustness with respect to the discontinuities in a without any restriction on a for any of the methods considered in this paper. In fact, tensor-valued $\mathbf{A}$ can also be considered, cf. Remark 5.18 below. However, this result is established in the dual norm $|||\cdot|||_\#$ and one only has global efficiency.

5 Some H^1-conforming methods, their mutual relations, and application of the estimates

The purpose of this section is to recall several classical numerical methods for problem (1.1a)–(1.1b) and their mutual relations. Using these relations, we infer the validity of (3.9) (and hence of our a posteriori error estimates) for all the considered methods.

5.1 Definitions

We start by giving the definitions.

Definition 5.1 (Weighted cell-centered finite volume method)**.** Let $\mathcal{D}_h$ be the Voronoï grid given by the vertices from $\mathcal{V}_h$, cf. Eymard *et al.* [26] (this requires that the vertices $V \in \mathcal{V}_h^{\rm ext}$ are suitably placed so that $\overline{\Omega} = \bigcup_{D\in\mathcal{D}_h} D$). Let next $\mathcal{N}(D)$ denote the set of "neighbors" of $D \in \mathcal{D}_h$, i.e., of such $E \in \mathcal{D}_h$ that $\sigma_{D,E} := \partial D \cap \partial E$ is such that $|\sigma_{D,E}| \neq 0$; in such a case, let $d_{D,E}$ stand for the Euclidean distance of the associated vertices V_D and V_E. Let finally a be piecewise constant on $\mathcal{D}_h$. Then the weighted cell-centered finite volume method for problem (1.1a)–(1.1b) reads: find $p_h = \sum_{D\in\mathcal{D}_h} p_D \psi_{V_D}$, with $p_D = 0$ for all $D \in \mathcal{D}_h^{\rm ext}$ so that $p_h \in X_h^0$, such that

$$-\sum_{E\in\mathcal{N}(D)} \{\!\{a\}\!\}_\omega \frac{|\sigma_{D,E}|}{d_{D,E}}(p_E - p_D) = (f,1)_D \qquad \forall D \in \mathcal{D}_h^{\rm int}. \tag{5.1}$$

The two basic choices for the weights in $\{\!\{a\}\!\}_\omega$ are the arithmetic averaging (2.4) and the harmonic averaging (2.5).

Definition 5.2 (Vertex-centered finite volume method)**.** Let the dual grid $\mathcal{D}_h$ consist of polygonal/polyhedral dual volumes and let a be piecewise constant on $\mathcal{T}_h$ so that a is not double-valued on $\mathcal{F}_h^{\rm int}$. Then the vertex-centered finite volume method for problem (1.1a)–(1.1b) reads: find $p_h \in X_h^0$ such that

$$-\langle a\nabla p_h \cdot \mathbf{n}, 1\rangle_{\partial D} = (f,1)_D \qquad \forall D \in \mathcal{D}_h^{\rm int}. \tag{5.2}$$

Definition 5.3 (Weighted vertex-centered finite volume method)**.** Let the dual grid $\mathcal{D}_h$ consist of polygonal/polyhedral dual volumes. Then we can design a weighted vertex-centered finite volume method for problem (1.1a)–(1.1b) as follows: find $p_h \in X_h^0$ such that

$$-\langle \{\!\{a\}\!\}_\omega \nabla p_h \cdot \mathbf{n}, 1\rangle_{\partial D} = (f,1)_D \qquad \forall D \in \mathcal{D}_h^{\rm int}. \tag{5.3}$$

Remark 5.4 (Arithmetic/harmonic averaging in the vertex-centered finite volume method). We first remark that when a is piecewise constant on $\mathcal{T}_h$, the above definition coincides with the standard Definition 5.2, which is known to lead to arithmetic-like averaging of a. When, however, a is piecewise constant on $\mathcal{D}_h$, then as in the cell-centered finite volume case, the two basic choices for the weights in $\{\!\{a\}\!\}_\omega$, (2.4) and (2.5), lead respectively to arithmetic and harmonic averaging of a.

Definition 5.5 (Finite element method)**.** The finite element method for problem (1.1a)–(1.1b) reads: find $p_h \in X_h^0$ such that

$$(a\nabla p_h, \nabla \psi_V)_{\mathcal{T}_V} = (f, \psi_V)_{\mathcal{T}_V} \qquad \forall V \in \mathcal{V}_h^{\rm int}. \tag{5.4}$$

Definition 5.6 (Finite element method with harmonic averaging)**.** Let the dual grid $\mathcal{D}_h$ consist of polygonal/polyhedral dual volumes and let a be piecewise constant on $\mathcal{D}_h$. Let us define $\tilde{a}$ by

$$\tilde{a}|_K = \left(\frac{(a^{-1},1)_K}{|K|}\right)^{-1} \qquad \forall K \in \mathcal{T}_h. \tag{5.5}$$

Then we can define a finite element method with harmonic averaging for problem (1.1a)–(1.1b) as: find $p_h \in X_h^0$ such that

$$(\tilde{a}\nabla p_h, \nabla \psi_V)_{\mathcal{T}_V} = (f, \psi_V)_{\mathcal{T}_V} \qquad \forall V \in \mathcal{V}_h^{\rm int}. \tag{5.6}$$

Remark 5.7 (Arithmetic/harmonic averaging in the finite element method). We remark that the difference between the matrices of (5.4) and (5.6) corresponds to the difference between the matrices of the piecewise linear nonconforming finite element method and that of the hybridization of the lowest-order Raviart–Thomas mixed finite element method in that the first ones use the arithmetic and the second ones use the harmonic averaging of the diffusion coefficient a, cf. [6]. In particular, by Definitions 5.5 and 5.6, one has in the finite element method the choice between the arithmetic and the harmonic averaging as in the finite volume one.

5.2 Equivalences

We are now ready to recall several equivalence results between the above methods.

Lemma 5.8 (Equivalence between matrices of finite elements and vertex-centered finite volumes)**.** *Let $D \in \mathcal{D}_h$ have Lipschitz-continuous boundaries and let $|\sigma \cap D| = |\sigma|/d$ for each $\sigma \in \mathcal{E}_h^{\rm int}$ with a vertex $V_D \in \mathcal{V}_h^{\rm int}$ and the associated $D \in \mathcal{D}_h^{\rm int}$. Let, moreover, a be piecewise constant on $\mathcal{T}_h$. Then, for all $p_h \in X_h^0$,*

$$(a\nabla p_h, \nabla \psi_{V_D})_{\mathcal{T}_{V_D}} = -\langle a\nabla p_h \cdot \mathbf{n}, 1\rangle_{\partial D} \qquad \forall D \in \mathcal{D}_h^{\rm int}. \tag{5.7}$$

Proof. Employing the Green theorem and the finite elements basis functions form, see [9, Lemma 3] for $d = 2$. □

Lemma 5.9 (Equivalence between matrices of finite elements and cell-centered finite volumes)**.** *Let $d = 2$, let $\mathcal{T}_h$ be Delaunay, that is let the circumcircle of each triangle does not contain any vertex in its interior, and let, moreover, no circumcenters of boundary triangles lie outside the domain Ω. Let $\mathcal{D}_h$ be the Voronoï grid given by the vertices from $\mathcal{V}_h$ and let $a = 1$. Then, for all $p_h \in X_h^0$,*

$$(\nabla p_h, \nabla \psi_{V_D})_{\mathcal{T}_{V_D}} = -\sum_{E \in \mathcal{N}(D)} \frac{|\sigma_{D,E}|}{d_{D,E}}(p_E - p_D) \qquad \forall D \in \mathcal{D}_h^{\rm int}.$$

Proof. See [26, Section III.12]. □

Remark 5.10 (Relation between finite elements and cell-centered finite volumes if $d = 3$). We remark that the above lemma does not generalize to three space dimensions, see, e.g., Letniowski [31] or Putti and Cordes [37].

Lemma 5.11 (Equivalence between right-hand sides of finite elements and finite volumes)**.** *Let $|D \cap K| = |K|/(d+1)$ for each $D \in \mathcal{D}_h^{\rm int}$ and each $K \in \mathcal{T}_{V_D}$. Let, moreover, f be piecewise constant on $\mathcal{T}_h$. Then*

$$(f, \psi_{V_D})_{\mathcal{T}_{V_D}} = (f, 1)_D \qquad \forall D \in \mathcal{D}_h^{\rm int}. \tag{5.8}$$

Proof. Straightforward using the condition $|D \cap K| = |K|/(d+1)$ for $D \in \mathcal{D}_h^{\rm int}$ and $K \in \mathcal{T}_{V_D}$ and a quadrature formula for linear functions on simplices. □

5.3 Consequences

The following corollaries are obvious consequences of the previous lemmas.

Corollary 5.12 (Equivalence between finite elements and vertex-centered finite volumes)**.** *Let the assumptions of Lemmas 5.8 and 5.11 be verified. Then the finite element method given by Definition 5.5 and the vertex-centered finite volume methods given by Definitions 5.2 and 5.3 produce the same discrete systems.*

Corollary 5.13 (Local conservativity of the finite element method on dual grids)**.** *Let the assumptions of Lemmas 5.8 and 5.11 be verified. Then the finite element method given by Definition 5.5 is locally conservative over the dual grid* $\mathcal{D}_h^{\rm int}$.

Corollary 5.14 (Equivalence between weighted cell- and vertex-centered finite volumes)**.** *Let* $d = 2$*, let* $\mathcal{T}_h$ *be Delaunay, let no circumcenters of boundary triangles lie outside the domain* Ω*, and let* $\mathcal{D}_h$ *be the Voronoï grid given by the vertices from* $\mathcal{V}_h$*. Let next* a *be piecewise constant on* $\mathcal{D}_h$*. Then the weighted cell-centered finite volume method given by Definition 5.1 and the weighted vertex-centered finite volume method given by Definition 5.3 produce the same discrete systems.*

5.4 Remarks

We finish this section by some additional remarks.

Remark 5.15 (Local conservativity of the finite element method). Corollary 5.13 should be understood in the following sense: First of all, equation (5.2) states that the sum of fluxes entering/leaving $D \in \mathcal{D}_h^{\rm int}$ equals the sources on this element. Secondly, rewriting $-\langle a\nabla p_h \cdot \mathbf{n}, 1\rangle_{\partial D}$ as $-\sum_{E\in\mathcal{N}(D)}\langle a\nabla p_h\cdot\mathbf{n}, 1\rangle_{\sigma_{D,E}}$ and noticing that the quantity $a\nabla p_h\cdot\mathbf{n}$ is single-valued on $\sigma_{D,E}$ under the given assumptions, local mass balance, in the sense that the mass leaving from one element (D) enters its neighbor (E), is likewise satisfied. Consequently, the finite element method is well locally mass conservative on $\mathcal{D}_h^{\rm int}$, even if it is not locally mass conservative on $\mathcal{T}_h$. Remark finally that the above assertions are only valid exactly if in particular a and f are piecewise constant on $\mathcal{T}_h$. In the general case, local mass conservativity on $\mathcal{D}_h$ only holds up to a numerical quadrature/data oscillation.

Remark 5.16 (Choice of the dual grids). In the above developments, a large freedom is left in what concerns the actual choice of the dual grids $\mathcal{D}_h$. The basic and most frequently used grid satisfying both the assumptions of Lemmas 5.8 and 5.11 is given by straight lines connecting the triangle barycentres through the midpoints of the edges of $\mathcal{T}_h$ if $d = 2$ and similarly if $d = 3$.

Remark 5.17 (Finite difference method). Let $\mathcal{D}_h$ consist of squares if $d = 2$ and cubes if $d = 3$. Then the finite difference method for problem (1.1a)–(1.1b) coincides with cell-centered finite volume one given by Definition 5.1, cf. Eymard *et al.* [26].

Remark 5.18 (Tensor-valued diffusion coefficients). In problem (1.1a)–(1.1b), we could also consider a tensor-valued diffusion coefficient $\mathbf{A}$ in place of the scalar-valued a. Definitions 5.5 and 5.6 would in this case contain $\mathbf{A}$ in place of a and similarly for Definitions 5.2 and 5.3. Then, for $\mathbf{A}$ piecewise constant on $\mathcal{T}_h$, Lemma 5.8 still holds true and similarly for Corollaries 5.12 and 5.13.

5.5 Application of the a posteriori error estimates

Through the above developments, we easily see that condition (3.9) is satisfied for the majority of the considered methods. In particular, the robustness lower bound result of Section 4.1 applies to the harmonic-weighted vertex-centered finite volume method (5.3) or the harmonic-weighted cell-centered finite volume method (5.1). Also, whenever f is piecewise constant on $\mathcal{T}_h$, the a posteriori error estimates for the finite element methods (5.4) or (5.6) are covered. It thus remains to check the case of finite element methods and general f. We do this for the finite element method (5.4) in the energy norm setting; the case (5.6) and the dual norm setting are similar.

Let f_h be given by $(f,1)_K/|K|$ on all $K \in \mathcal{T}_h$. Following [42], we then have:

Theorem 5.19 (Guaranteed a posteriori error estimate for the finite element method)**.** *Let* p *be the weak solution of problem* (1.1a)–(1.1b)*, let* p_h *be its finite element approximation given by* (5.4)*,*

let $\tilde{p}$ be the weak solution of problem (1.1a)–(1.1b) with f replaced by f_h, and let $\tilde{p}_h$ be its finite element approximation. Then

$$|||p - p_h||| \le |||\tilde{p} - \tilde{p}_h||| + 2\left\{\sum_{K\in\mathcal{T}_h} \eta_{\mathrm{Osc},K}^2\right\}^{\frac{1}{2}},$$

where

$$\eta_{\mathrm{Osc},K} := C_{\mathrm{P},K}^{\frac{1}{2}} \frac{h_K}{c_{a,K}^{\frac{1}{2}}} \|f - f_K\|_K \qquad K \in \mathcal{T}_h.$$

Proof. The triangle inequality implies

$$|||p - p_h||| \le |||p - \tilde{p}||| + |||\tilde{p} - \tilde{p}_h||| + |||\tilde{p}_h - p_h|||.$$

By the same reasoning as in the proof of Theorem 3.1, using the definitions of the weak solutions, and finally similarly as in the proof of Theorem 3.4,

$$\begin{aligned} |||p - \tilde{p}||| &= \sup_{\varphi\in H_0^1(\Omega),\, |||\varphi|||=1} (a\nabla(p-\tilde{p}), \nabla\varphi) = \sup_{\varphi\in H_0^1(\Omega),\, |||\varphi|||=1} (f - f_h, \varphi) \\ &\le \sup_{\varphi\in H_0^1(\Omega),\, |||\varphi|||=1} \sum_{K\in\mathcal{T}_h} (f - f_K, \varphi - \varphi_K)_K \le \left\{\sum_{K\in\mathcal{T}_h} \eta_{\mathrm{Osc},K}^2\right\}^{\frac{1}{2}}. \end{aligned}$$

Estimating the term $|||\tilde{p}_h - p_h|||$ similarly in a discrete setting concludes the proof. □

We end this section by the following remark:

Remark 5.20 (Local efficiency and robustness of the a posteriori error estimates for the finite element methods (5.4) and (5.6)). If a is piecewise constant on $\mathcal{T}_h$ and under the other assumptions of Lemmas 5.8 and 5.11, we have by Corollary 5.12 that Remark 4.7 holds true also for the finite element method (5.4). On the other hand, when a is piecewise constant on $\mathcal{D}_h$, the finite element method with harmonic averaging (5.6) leads to a scheme which is very close to the harmonic-weighted vertex-centered finite volume method (5.3). Indeed, as $|D \cap K| = |K|/3$ for $D \in \mathcal{D}_h$ associated with one of the vertices of $K \in \mathcal{T}_h$ for the meshes of Section 2.1, the coefficient $\tilde{a}|_K$ from (5.5) is given by the harmonic averaging of the three values a_D, a_E, and a_F that a takes at the three dual volumes D, E, and F associated with the vertices of K. Consequently, for f piecewise constant on $\mathcal{T}_h$, (5.6) gives (5.3) where $\{\!\{a\}\!\}_\omega$ is now the harmonic average of a_D, a_E, and a_F. To obtain a guaranteed estimate, one defines $\mathbf{t}_h \in \mathbf{RTN}(\mathcal{S}_h)$ by fixing $\mathbf{t}_h \cdot \mathbf{n}$ on the boundary of $D \in \mathcal{D}_h^{\mathrm{int}}$ by $-\tilde{a}\nabla p_h \cdot \mathbf{n}$ and by (3.10) for the other sides of $\mathcal{S}_h$, while separating the oscillations in f as in Theorem 5.19. Robustness can then be proved as in Theorem 4.1.

6 Numerical experiments

We present in this section the results of several numerical experiments.

6.1 A one-dimensional example with a smooth solution

We begin with a one-dimensional model problem

$$\begin{aligned} -p'' &= \pi^2 \sin(\pi x) \qquad \text{in }]0,1[, \\ p &= 0 \quad \text{in } 0, 1. \end{aligned}$$

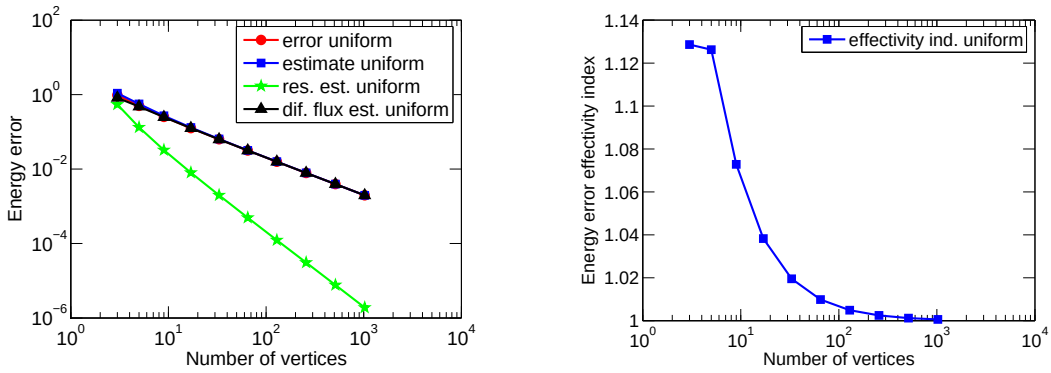

Figure 2: Estimated and actual energy error (left) and corresponding effectivity index (right) for the one-dimensional example

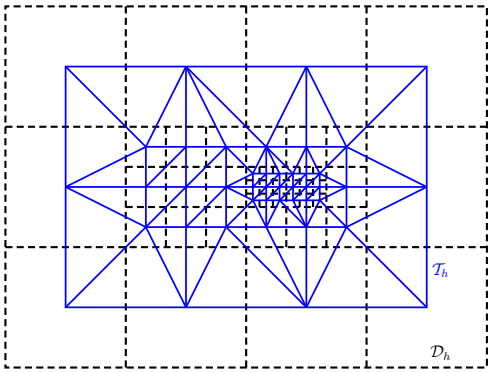

Figure 3: Example of a given nonmatching dual mesh $\mathcal{D}_h$ and the corresponding primal triangular mesh $\mathcal{T}_h$ for the harmonic-weighted vertex-centered finite volume method (5.3)

The exact solution is smooth and given by $p(x) = \sin(\pi x)$. We consider the vertex-centered finite volume method (5.2) on a series of uniformly refined meshes and construct a one-dimensional equivalent of the equilibrated field $\mathbf{t}_h$ given by (3.10). The results are reported in Figure 2. It turns out that in this one-dimensional setting, one actually has $(\nabla\cdot\mathbf{t}_h, 1)_K = (f, 1)_K$ for all $K \in \mathcal{S}_h$ instead of (3.2) and hence the residual estimators $\eta_{\mathrm{R},D}$ represent a contribution of higher order and are only significant on coarsest meshes. We also observe asymptotic exactness in the right part of Figure 2. Define the experimental order of convergence (e.o.c.) by

$$\text{e.o.c.} := \frac{\log(e_N) - \log(e_{N-1})}{\frac{1}{d}\log|\mathcal{V}_{N-1}| - \frac{1}{d}\log|\mathcal{V}_N|};$$

here e_N is the error on the last mesh, e_{N-1} is the error on the last but one mesh, and $|\mathcal{V}_N|$ and $|\mathcal{V}_{N-1}|$ denote the corresponding number of vertices. The e.o.c. is equal to 1.001 here.

6.2 Robust energy norm estimates for the vertex-centered finite volume method with harmonic averaging

We consider here a model problem taken from [40], where $\Omega = (-1,1)\times(-1,1)$ is divided into four subdomains Ω_i along the Cartesian axes (the subregion $\{x>0, y>0\}\cap\Omega$ is denoted by Ω_1 and the subsequent numbering is done counterclockwise) and a is constant and equal to a^i in Ω_i.

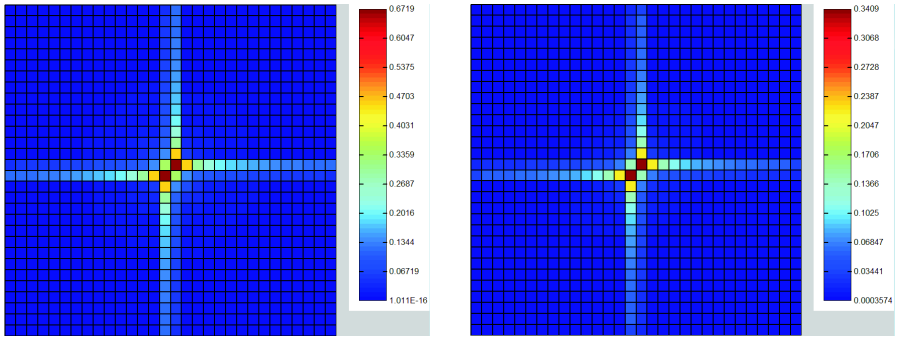

Figure 4: Estimated (left) and actual (right) energy error distribution on a uniformly refined mesh, $\alpha = 0.535$, harmonic-weighted vertex-centered finite volume method (5.3)

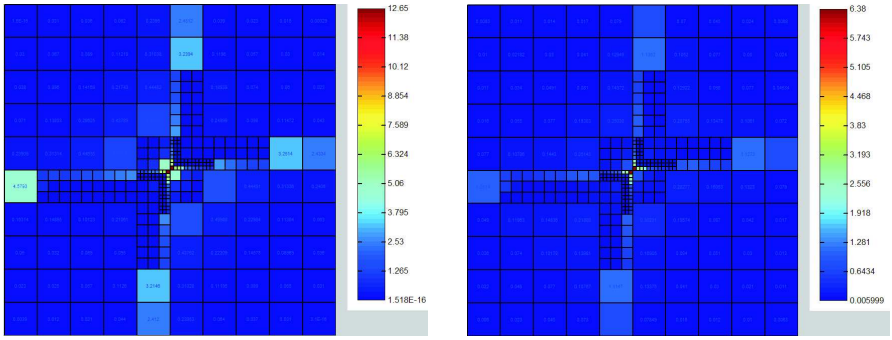

Figure 5: Estimated (left) and actual (right) energy error distribution on an adaptively refined mesh, $\alpha = 0.127$, harmonic-weighted vertex-centered finite volume method (5.3)

Supposing in addition that $f = 0$, analytical solution writing

$$p(r, \theta) = r^\alpha (a_i \sin(\alpha\theta) + b_i \cos(\alpha\theta))$$

in each Ω_i can be found. Here (r, θ) are the polar coordinates in Ω, a_i and b_i are constants depending on Ω_i, and α is a parameter. This solution is continuous across the interfaces but only the normal component of its flux $\mathbf{u} = -\mathbf{S}\nabla p$ is continuous; it exhibits a singularity at the origin and it only belongs to $H^{1+\alpha}(\Omega)$. We assume Dirichlet boundary conditions given by this solution and consider two sets of the coefficients. In the first one, $a^1 = a^3 = 5$, $a^2 = a^4 = 1$, $\alpha = 0.53544095$, and in the second one, $a^1 = a^3 = 100$, $a^2 = a^4 = 1$, $\alpha = 0.12690207$. The corresponding values of a_i, b_i can be found in [40, 48].

In order to get robust a posteriori error estimates in the energy norm, we know from Theorem 4.1 that a has to be piecewise constant on $\mathcal{D}_h$. If, however, we would first construct a simplicial mesh $\mathcal{T}_h$ of Ω and then a dual grid $\mathcal{D}_h$ as in Section 2.1, it would be very difficult to keep the dual mesh aligned with the inhomogeneities, especially for adaptive refinement. A possible solution is to first define the dual mesh $\mathcal{D}_h$ and only then the primal one $\mathcal{T}_h$. On the resulting couple of grids $\mathcal{D}_h$, $\mathcal{T}_h$, we then use the weighted vertex-centered finite volume method (5.3). Recall that on square grids (and their uniform refinements), this method is equivalent to the weighted cell-centered finite volume one, cf. Corollary 5.14, as well as to the finite difference one, cf. Remark 5.17. The advantage of the scheme (5.3) is that it can be used also when the original square grid has been locally refined (into a nonmatching grid) as in Figure 3. Note however that the symmetry of this scheme is then lost. We remark that the present methodology works also for the finite element method with harmonic averaging (5.5), which stays symmetric.

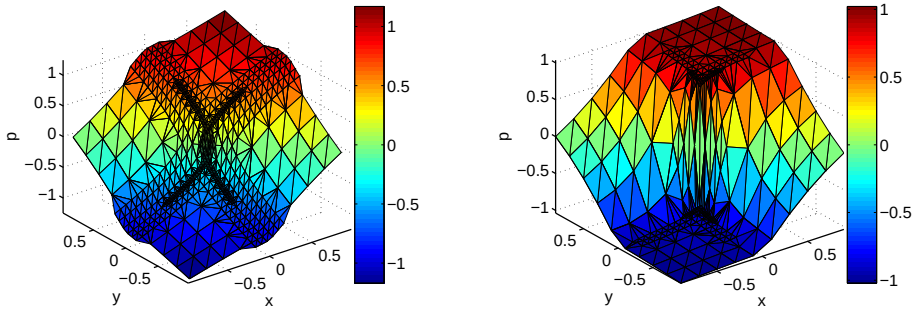

Figure 6: Approximate solutions on adaptively refined meshes, $\alpha = 0.535$ (left) and $\alpha = 0.127$ (right), harmonic-weighted vertex-centered finite volume method (5.3)

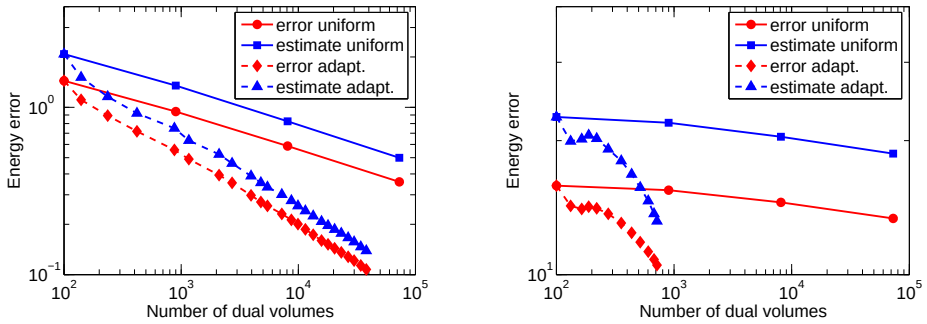

Figure 7: Estimated and actual energy errors for $\alpha = 0.535$ (left) and $\alpha = 0.127$ (right), harmonic-weighted vertex-centered finite volume method (5.3), estimates with local minimization (3.11)

We in Figure 4 present the predicted and actual distribution of the error for $\alpha = 0.535$ and uniform mesh refinement, using the estimators of Theorem 3.4 on the dual mesh $\mathcal{D}_h$ and with $\mathbf{t}_h$ given by (3.10) (the interpolation error on nonhomogeneous Dirichlet boundary conditions is neglected). A similar comparison, this time for adaptive mesh refinement and $\alpha = 0.127$, is shown in Figure 5. A square cell of the original dual mesh is refined into 9 identical subsquares if the estimated energy error is greater than 50% of the maximum of the estimators. We can see that in both cases the predicted error distribution is excellent and that in particular, the singularity at the origin is well detected. These results clearly illustrate the robust local lower bound of Theorem 4.1. We finally in Figure 6 give examples of the approximate solutions on the adaptively refined meshes in both cases; the strength of the singularity in the second case is quite obvious.

Knowing precisely the error distribution and refining adaptively the meshes, the next step is to check whether this leads to an increased efficiency of the calculations. This is illustrated in Figure 7, from which it is evident that one can achieve a given precision with much fewer elements using adaptive mesh refinement based on our estimator. Here, the error in the energy norm (2.10) is approximated with a 7-point quadrature formula in each subtriangle $K \in \mathcal{S}_D$. In the code TALISMAN, which we use for numerical computations in this section, at most 9 levels of refinement can be used. This technical limitation is the reason why we in the adaptive case and for $\alpha = 0.127$ only present results with at most 716 dual volumes—this maximal refinement level is achieved near the origin but the maximal error is still located there. For $\alpha = 0.535$, the e.o.c. for uniform refinement was 0.449 and for the adaptive one 1.006. For $\alpha = 0.127$, these values were respectively 0.0757 and 1.024. Following [7], the somewhat slower convergence rate for uniform

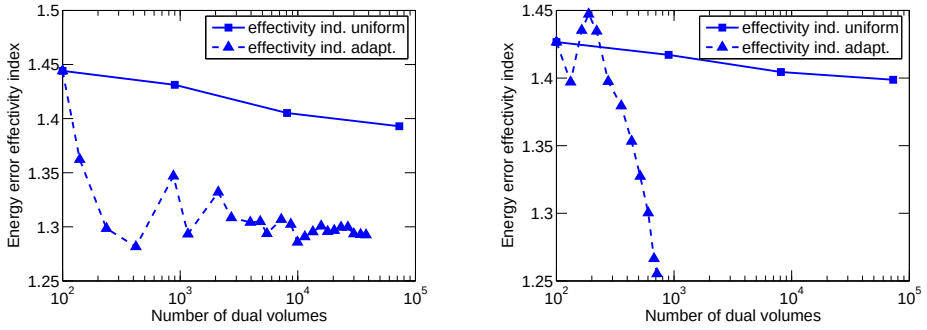

Figure 8: Energy error effectivity indices for $\alpha = 0.535$ (left) and $\alpha = 0.127$ (right), harmonic-weighted vertex-centered finite volume method (5.3), estimates with local minimization (3.11)

refinement (compare with the finite element case below) in the energy norm is related to the fact that the coefficient a is not aligned with the mesh $\mathcal{T}_h$ on which we reconstruct the approximate solution p_h.

Finally, in Figure 8, we give the effectivity indices using the local minimization approach described in Section 3.3.3. We can clearly observe a confirmation of the robustness of our estimators: whereas the inhomogeneity ratio rises from 5 to 100, the effectivity indices stay et the level of 1.4 for uniform refinement and improve for adaptive refinement. Moreover, the local minimization of Section 3.3.3 allows for almost asymptotic exactness, and this even in the case of discontinuous coefficients and singular solutions.

6.3 Energy estimates for the finite element method based on local Neumann/ Dirichlet mixed finite element problems

For the same model problem as in the previous section, we present here the results for the finite element method (5.4) with the energy error estimators of Theorem 3.4 based on local Neumann/Dirichlet mixed finite element problems of Section 3.3.4 (thus $\mathcal{D}_h^{\mathrm{int},*} = \mathcal{S}_h$ and $\mathcal{D}_h^{\mathrm{ext},*} = \emptyset$ in Theorem 3.4). The initial mesh consisted of 24 right-angled triangles, conforming with the 4 subdomains (for the corresponding mesh $\mathcal{S}_h$, we refer to Figure 11).

Figure 9 shows the estimated and actual energy errors using the estimators based on the local Neumann/Dirichlet mixed finite element problems described in Section 3.3.4. For $\alpha = 0.535$, the e.o.c. for uniform refinement is 0.537 and for the adaptive one 0.999; for $\alpha = 0.127$, these values are, respectively, 0.172 and 0.946. This is fully in agreement with the smoothness of the weak solutions (recall that $p \in H^{1+\alpha}(\Omega)$) for the uniform refinement and shows optimal behavior of the adaptive refinement strategy. For $\alpha = 0.127$, the adaptive refinement is stopped for roughly 700 elements as the diameter of the smallest triangles near the origin reaches 10^{-16} which is the computer double precision.

The corresponding effectivity indices are presented in Figure 10. As predicted by the theory, we can observe in comparison with Figure 8 that the estimates are no more robust with respect to the discontinuities in a. The effectivity index is around 1.6 for $\alpha = 0.535$ and 4.7 for $\alpha = 0.127$, although it gets down to roughly 1.27 for adaptive mesh refinement. As seen from Figure 11, the biggest overestimation appears around the center and the error distribution is no more predicted accurately (compare with Figures 4 and 5). The two forthcoming sections improve on these points.

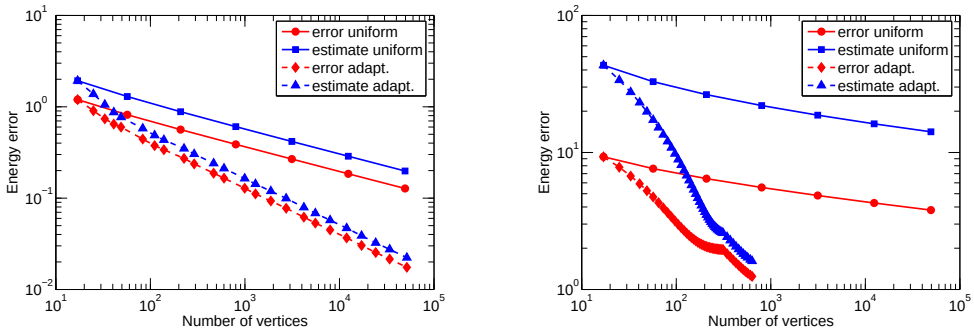

Figure 9: Estimated and actual energy errors for $\alpha = 0.535$ (left) and $\alpha = 0.127$ (right), finite element method (5.4), estimates by local Neumann/Dirichlet mixed finite element problems (3.12)

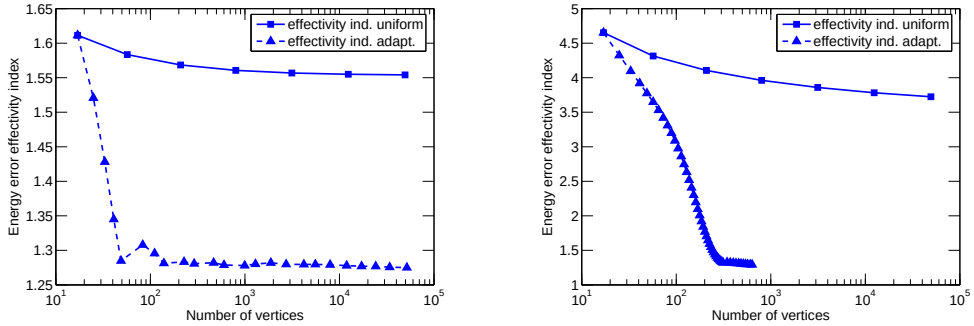

Figure 10: Energy error effectivity indices for $\alpha = 0.535$ (left) and $\alpha = 0.127$ (right), finite element method (5.4), estimates by local Neumann/Dirichlet mixed finite element problems (3.12)

6.4 Robust dual norm estimates for the finite element method

With the same setting as in the previous section, we now switch to the estimates in the dual norm (2.11) of Corollary 3.5.

Figure 12 reports the estimated and actual dual error; here "error up" means the computable upper bound on the dual error from (2.12), whereas "error down" means the computable lower bound from (2.12). In the dual error upper bound, for $\alpha = 0.535$, the e.o.c. for uniform refinement

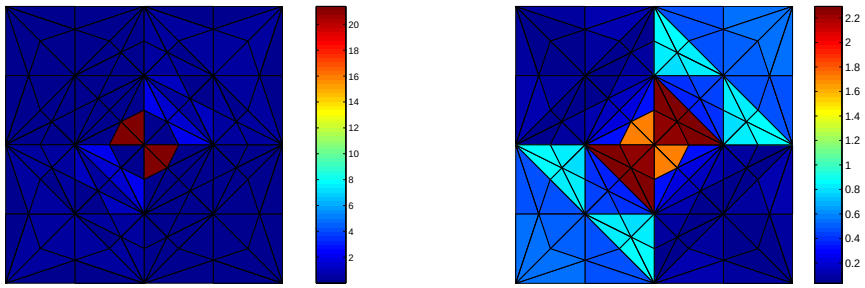

Figure 11: Estimated (left) and actual (right) energy error distribution on $\mathcal{S}_h$ for $\alpha = 0.127$, finite element method (5.4), estimates by local Neumann/Dirichlet mixed finite element problems (3.12)

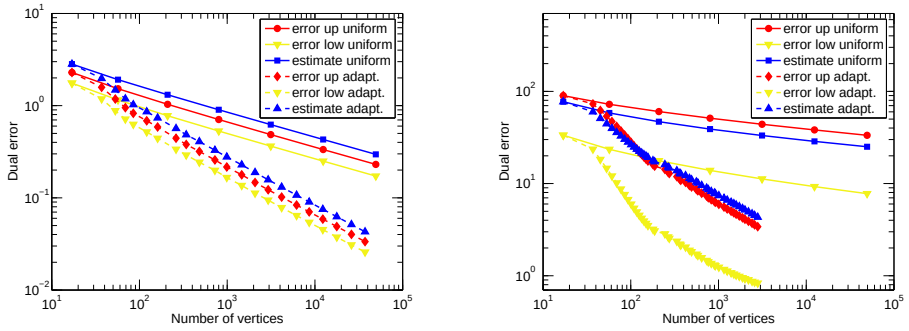

Figure 12: Estimated and actual dual errors for $\alpha = 0.535$ (left) and $\alpha = 0.127$ (right), finite element method (5.4), estimates by local Neumann/Dirichlet mixed finite element problems (3.12)

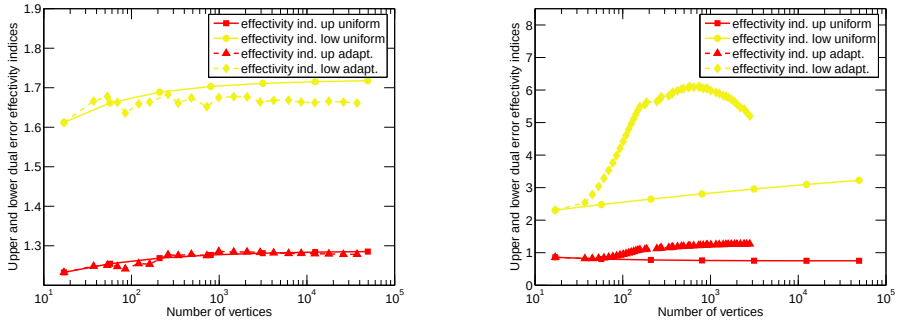

Figure 13: Dual error effectivity indices for $\alpha = 0.535$ (left) and $\alpha = 0.127$ (right), finite element method (5.4), estimates by local Neumann/Dirichlet mixed finite element problems (3.12)

is 0.539 and for the adaptive one 1.017; for $\alpha = 0.127$, these values are, respectively, 0.195 and 1.109. In Figure 13, we then report the corresponding effectivity indices. As predicted by Theorem 4.4, the estimates in the dual norm are fully robust. In particular, the effectivity index in the dual error upper bound is stable around the optimal value of 1; note that its values below 1 are possible since the estimates are derived for the dual norm and not for this upper bound. One conclusion from Figures 12 and 13 is that now the nonrobustness has been shifted to the gap between the computable upper and lower bounds for the dual error. Finally, Figure 14 shows the predicted dual error distribution and actual dual upper bound error distribution which reveals excellent (note in particular that there is no gap in the scales of the figures, contrarily to the energy setting of Figure 11).

6.5 Energy norm estimates based on local refinements of individual dual volumes

We finally come back shortly to the energy norm framework of Section 6.3. The idea is to solve the mixed finite element minimization problem (3.12) on a local refinement of the mesh $\mathcal{S}_D$ in individual dual volumes $D \in \mathcal{D}_h$, with the hope to decrease the error estimates in individual dual volumes. The local refinement is driven by the quantity $\|a^{\frac{1}{2}}\nabla p_h + a^{-\frac{1}{2}}\mathbf{t}_h\|_K$ on each element K of the local refinement of $\mathcal{S}_D$. We refine here only the central dual volume, as only in this dual volume the overestimation dependent on the jumps in a occurs. Figure 15 shows that this indeed enables to substantially decrease the effectivity indices (to be compared with Figure 10),

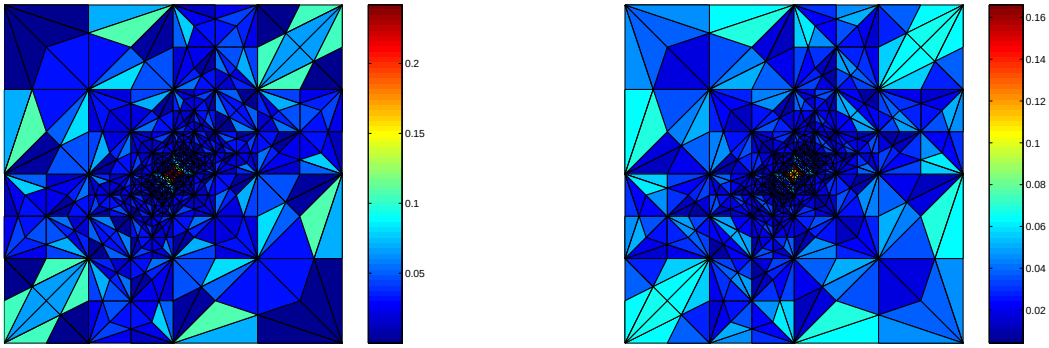

Figure 14: Estimated (left) and actual (right) dual error distribution on $\mathcal{S}_h$ for $\alpha = 0.535$, finite element method (5.4), estimates by local Neumann/Dirichlet mixed finite element problems (3.12)

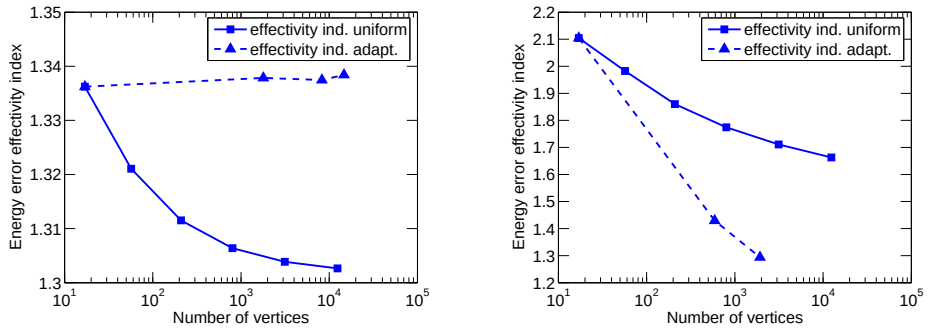

Figure 15: Energy error effectivity indices for $\alpha = 0.535$ (left) and $\alpha = 0.127$ (right), finite element method (5.4), estimates by local refinements of individual dual volumes

although robustness is only achieved for $\alpha = 0.535$; for $\alpha = 0.127$, still an overestimation by a factor of 2.1 appears. Such a procedure also allows to predict much more precisely the error distribution, see the right part of Figure 16, in comparison with Figure 11. Another possible use of the independent refinement of only those dual volumes where the error indicator is large is to include the obtained local refinement to the mesh of the entire domain. Such a procure is illustrated in the left part of Figure 16, and, in the present case, allows to substantially improve the classical local refinement illustrated in the right part of Figure 10. Note that only two steps of the local refinement cycle on the global level allow to achieve the same precision as 49 steps in Section 6.3. Finally, the predicted and actual error distribution in the locally refined central dual volume is shown in Figure 17. It indicates that with the boundary conditions on ∂D given by $-\{\!\{a\nabla p_h \cdot \mathbf{n}_\sigma\}\!\}$, one cannot obtain a robust estimate and correct error distribution in the energy norm setting for the finite element method (5.4) even with such a local refinement of one dual volume; a larger domain would probably be necessary, indicating the nonlocality of the error distribution. Thus, in confirmation of the theory of Section 4, only the approaches of Sections 6.2 and 6.4 seem to give robust estimates (and correct error distribution).

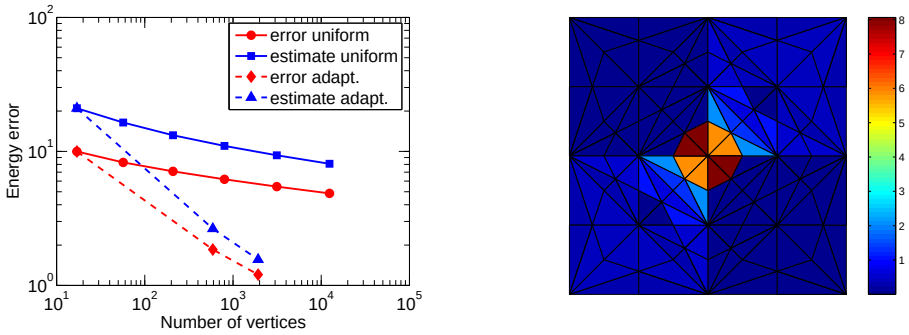

Figure 16: Estimated and actual energy error for $\alpha = 0.127$ (left) and estimated energy error distribution, finite element method (5.4), estimates by local refinements of ind. dual volumes

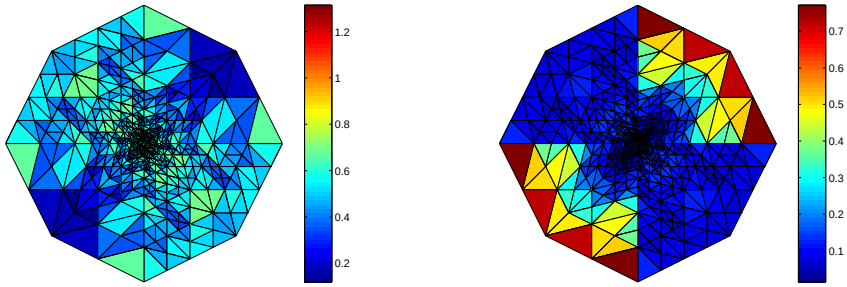

Figure 17: Estimated (left) and actual (right) energy error distribution on the locally refined central dual volume, $\alpha = 0.127$, finite element method (5.4)

References

[1] Ainsworth, M. Robust a posteriori error estimation for nonconforming finite element approximation. *SIAM J. Numer. Anal. 42*, 6 (2005), 2320–2341.

[2] Ainsworth, M. A synthesis of a posteriori error estimation techniques for conforming, nonconforming and discontinuous Galerkin finite element methods. In *Recent advances in adaptive computation*, vol. 383 of *Contemp. Math.* Amer. Math. Soc., Providence, RI, 2005, pp. 1–14.

[3] Ainsworth, M., and Oden, J. T. *A posteriori error estimation in finite element analysis.* Pure and Applied Mathematics (New York). Wiley-Interscience [John Wiley & Sons], New York, 2000.

[4] Angermann, L. Balanced a posteriori error estimates for finite-volume type discretizations of convection-dominated elliptic problems. *Computing 55*, 4 (1995), 305–323.

[5] Arbogast, T., and Chen, Z. On the implementation of mixed methods as nonconforming methods for second-order elliptic problems. *Math. Comp. 64*, 211 (1995), 943–972.

[6] Arnold, D. N., and Brezzi, F. Mixed and nonconforming finite element methods: implementation, postprocessing and error estimates. *RAIRO Modél. Math. Anal. Numér. 19*, 1 (1985), 7–32.

[7] Babuška, I. personnal communication. 2008.

[8] Babuška, I., and Rheinboldt, W. C. Error estimates for adaptive finite element computations. *SIAM J. Numer. Anal. 15*, 4 (1978), 736–754.

[9] Bank, R. E., and Rose, D. J. Some error estimates for the box method. *SIAM J. Numer. Anal. 24*, 4 (1987), 777–787.

[10] Bank, R. E., and Weiser, A. Some a posteriori error estimators for elliptic partial differential equations. *Math. Comp. 44*, 170 (1985), 283–301.

[11] Bebendorf, M. A note on the Poincaré inequality for convex domains. *Z. Anal. Anwendungen 22*, 4 (2003), 751–756.

[12] Bernardi, C., and Verfürth, R. Adaptive finite element methods for elliptic equations with non-smooth coefficients. *Numer. Math. 85*, 4 (2000), 579–608.

[13] Braess, D. *Finite elements*, third ed. Cambridge University Press, Cambridge, 2007. Theory, fast solvers, and applications in elasticity theory, Translated from the German by Larry L. Schumaker.

[14] Braess, D., Pillwein, V., and Schöberl, J. Equilibrated residual error estimates are p-robust. *Comput. Methods Appl. Mech. Engrg. 198*, 13-14 (2009), 1189–1197.

[15] Braess, D., and Schöberl, J. Equilibrated residual error estimator for edge elements. *Math. Comp. 77*, 262 (2008), 651–672.

[16] Brezzi, F., and Fortin, M. *Mixed and hybrid finite element methods*, vol. 15 of *Springer Series in Computational Mathematics*. Springer-Verlag, New York, 1991.

[17] Cai, Z., and Zhang, S. Recovery-based error estimator for interface problems: conforming linear elements. *SIAM J. Numer. Anal. 47*, 3 (2009), 2132–2156.

[18] Carstensen, C., and Funken, S. A. Constants in Clément-interpolation error and residual based a posteriori error estimates in finite element methods. *East-West J. Numer. Math. 8*, 3 (2000), 153–175.

[19] Chaillou, A. L., and Suri, M. Computable error estimators for the approximation of nonlinear problems by linearized models. *Comput. Methods Appl. Mech. Engrg. 196*, 1-3 (2006), 210–224.

[20] Cheddadi, I., Fučík, R., Prieto, M. I., and Vohralík, M. Computable a posteriori error estimates in the finite element method based on its local conservativity: improvements using local minimization. *ESAIM Proc. 24* (2008), 77–96.

[21] Cheddadi, I., Fučík, R., Prieto, M. I., and Vohralík, M. Guaranteed and robust a posteriori error estimates for singularly perturbed reaction–diffusion problems. *M2AN Math. Model. Numer. Anal. 43*, 5 (2009), 867–888.

[22] Chen, Z., and Dai, S. On the efficiency of adaptive finite element methods for elliptic problems with discontinuous coefficients. *SIAM J. Sci. Comput. 24*, 2 (2002), 443–462.

[23] Destuynder, P., and Métivet, B. Explicit error bounds in a conforming finite element method. *Math. Comp. 68*, 228 (1999), 1379–1396.

[24] Ern, A., Stephansen, A. F., and Vohralík, M. Improved energy norm a posteriori error estimation based on flux reconstruction for discontinuous Galerkin methods. Preprint R07050, Laboratoire Jacques-Louis Lions & HAL Preprint 00193540 version 1 (14-11-2007), Université Paris 6 and Ecole des Ponts, 2007.

[25] Ern, A., and Vohralík, M. Flux reconstruction and a posteriori error estimation for discontinuous Galerkin methods on general nonmatching grids. *C. R. Math. Acad. Sci. Paris 347* (2009), 441–444.

[26] Eymard, R., Gallouët, T., and Herbin, R. Finite volume methods. In *Handbook of Numerical Analysis, Vol. VII*. North-Holland, Amsterdam, 2000, pp. 713–1020.

[27] Fierro, F., and Veeser, A. A posteriori error estimators, gradient recovery by averaging, and superconvergence. *Numer. Math. 103*, 2 (2006), 267–298.

[28] Korotov, S. Two-sided a posteriori error estimates for linear elliptic problems with mixed boundary conditions. *Appl. Math. 52*, 3 (2007), 235–249.

[29] Ladevèze, P. *Comparaison de modèles de milieux continus*. Ph.D. thesis, Université Pierre et Marie Curie (Paris 6), 1975.

[30] Ladevèze, P., and Leguillon, D. Error estimate procedure in the finite element method and applications. *SIAM J. Numer. Anal. 20*, 3 (1983), 485–509.

[31] Letniowski, F. W. Three-dimensional Delaunay triangulations for finite element approximations to a second-order diffusion operator. *SIAM J. Sci. Statist. Comput. 13*, 3 (1992), 765–770.

[32] Luce, R., and Wohlmuth, B. I. A local a posteriori error estimator based on equilibrated fluxes. *SIAM J. Numer. Anal. 42*, 4 (2004), 1394–1414.

[33] Neittaanmäki, P., and Repin, S. *Reliable methods for computer simulation*, vol. 33 of *Studies in Mathematics and its Applications*. Elsevier Science B.V., Amsterdam, 2004. Error control and a posteriori estimates.

[34] Payne, L. E., and Weinberger, H. F. An optimal Poincaré inequality for convex domains. *Arch. Rational Mech. Anal. 5* (1960), 286–292.

[35] Petzoldt, M. A posteriori error estimators for elliptic equations with discontinuous coefficients. *Adv. Comput. Math. 16*, 1 (2002), 47–75.

[36] Prager, W., and Synge, J. L. Approximations in elasticity based on the concept of function space. *Quart. Appl. Math. 5* (1947), 241–269.

[37] Putti, M., and Cordes, C. Finite element approximation of the diffusion operator on tetrahedra. *SIAM J. Sci. Comput. 19*, 4 (1998), 1154–1168.

[38] Repin, S. *A posteriori estimates for partial differential equations*, vol. 4 of *Radon Series on Computational and Applied Mathematics*. Walter de Gruyter GmbH & Co. KG, Berlin, 2008.

[39] Repin, S. I. A posteriori error estimation for nonlinear variational problems by duality theory. *Zap. Nauchn. Sem. S.-Peterburg. Otdel. Mat. Inst. Steklov. (POMI) 243*, Kraev. Zadachi Mat. Fiz. i Smezh. Vopr. Teor. Funktsii. 28 (1997), 201–214, 342.

[40] Rivière, B., Wheeler, M. F., and Banas, K. Part II. Discontinuous Galerkin method applied to single phase flow in porous media. *Comput. Geosci. 4*, 4 (2000), 337–349.

[41] Roberts, J. E., and Thomas, J.-M. Mixed and hybrid methods. In *Handbook of Numerical Analysis, Vol. II.* North-Holland, Amsterdam, 1991, pp. 523–639.

[42] Schöberl, J. personnal communication. 2009.

[43] Synge, J. L. *The hypercircle in mathematical physics: a method for the approximate solution of boundary value problems.* Cambridge University Press, New York, 1957.

[44] Vejchodský, T. Guaranteed and locally computable a posteriori error estimate. *IMA J. Numer. Anal. 26*, 3 (2006), 525–540.

[45] Verfürth, R. *A review of a posteriori error estimation and adaptive mesh-refinement techniques.* Teubner-Wiley, Stuttgart, 1996.

[46] Verfürth, R. Robust a posteriori error estimates for stationary convection-diffusion equations. *SIAM J. Numer. Anal. 43*, 4 (2005), 1766–1782.

[47] Vohralík, M. On the discrete Poincaré–Friedrichs inequalities for nonconforming approximations of the Sobolev space H^1. *Numer. Funct. Anal. Optim. 26*, 7–8 (2005), 925–952.

[48] Vohralík, M. A posteriori error estimates for lowest-order mixed finite element discretizations of convection-diffusion-reaction equations. *SIAM J. Numer. Anal. 45*, 4 (2007), 1570–1599.

[49] Vohralík, M. A posteriori error estimation in the conforming finite element method based on its local conservativity and using local minimization. *C. R. Math. Acad. Sci. Paris 346*, 11–12 (2008), 687–690.

[50] Vohralík, M. Two types of guaranteed (and robust) a posteriori estimates for finite volume methods. In *Finite Volumes for Complex Applications V.* ISTE and John Wiley & Sons, London, UK and Hoboken, USA, 2008, pp. 649–656.

[51] Xu, J., Zhu, Y., and Zou, Q. New adaptive finite volume methods and convergence analysis. Preprint AM296, Mathematics Department, Penn State, 2006.

[52] Zienkiewicz, O. C., and Zhu, J. Z. A simple error estimator and adaptive procedure for practical engineering analysis. *Internat. J. Numer. Methods Engrg. 24*, 2 (1987), 337–357.